Master's thesis

NTNU
Norwegian University of Science and Technology
Faculty of Engineering
Department of Civil and Environmental Engineering

Wendwesen Worku Lemma

Physical modelling of dam overtopping from waves induced by porous slides

Master's thesis in Hydropower Development
Supervisor: Fjola Gudrun Sigtryggsdottir
June 2019

NTNU
Norwegian University of
Science and Technology

Wendwesen Worku Lemma

Physical modelling of dam overtopping from waves induced by porous slides

Master's thesis in Hydropower Development
Supervisor: Fjola Gudrun Sigtryggsdottir
June 2019

Norwegian University of Science and Technology
Faculty of Engineering
Department of Civil and Environmental Engineering

NTNU
Norwegian University of
Science and Technology

NTNU

M.Sc. THESIS ASSIGNMENT

Candidate: Wendwesen Worku Lemma

Title: Physical modelling of dam overtopping from waves induced by porous slides

1. Background

Landslide generated impulse waves may cause damages as they run-up shores, or against dams retaining a reservoir. Large such waves may overtop dams with hazardous consequences for the downstream area. The hazard may be intensified in the case of an embankment dam, considering that this may erode and even completely fail during such extreme loading conditions, thereby releasing more water from the reservoir.

It was with this background, that the Norwegian Water Resources and Energy Directorate (NVE) in collaboration with NTNU, initiated a research program on the impacts of landslide generated wave action on embankment dams, particularly rockfill dams. For this, an experimental work has been carried out on a physical model in the hydraulic laboratory at NTNU.

In 2014, experimental tests have been carried out for different landslide scenarios, and dam parameters. The physical processes and interaction between the landslide generated waves and dam overtopping was studied. A comparison was also made between the results obtained from the experimental test with results from the computational method recommended by Heller et al. (2009).

As a continuation of the project, an experimental study was also carried out in 2015 and spring 2016 using the model in the hydraulic laboratory. The experimental test was mainly focused on the slide volume and dam characteristics and was performed under several different scenarios by varying the parameters of the slide volume, the reservoir water levels, and the upstream dam face slope, and the dam alignment. A test program was also carried out with rough and smooth upstream dam face, respectively.

During the fall 2016, and the years 2017 and 2018, a study into the different parameter was continued, varying also the speed of the landslide. Additionally, the ramp for the landslide was moved to the other side of the test basin late 2016 to investigate potential laboratory effects in the previous setup.

In general, the above mentioned studies have enhanced the understanding on the effect of the landslide generated waves and dam parameters. However, the new landslide setup from 2016 has only been tested with solid landslide blocks (no porosity) and two different freeboard conditions. Thus, the model provides opportunity for further studies to be conducted with different freeboard and landslide characteristics, such as porous landslide blocks. Mountainous terrains can be affected by different landslide types, e.g. earth slides and rockslides, this is e.g. the case in both Ethiopia and Norway. The porous landslide blocks aiming at modelling granular slides, whereas the solid blocks would represent rockslides.

2. Work description

The thesis will be composed of a number of tasks related to assessing relevant literature and preparing and running an experimental study on the existing physical model. The main objective of the study is to use the scale model in the hydraulic laboratory, in order to investigate the effect of landslide generated waves on embankment dams.

The main focus will be on using the porous landslide blocks and comparing the results to previous studies using the solid landslide blocks. This knowledge should contribute to the process of developing a method to calculate the size of the overtopping over an embankment dam as a result of landslide generated wave in reservoirs.

2.1 The specific tasks are as follows

1. Review current literature: An important aspect of the review will be to investigate previous studies on landslide generated wave impacts on embankment dam and study the governing parameters, their characteristics and interaction. Also, to study the literature on waves generated by solid versus granular landslides.

2. Select in co-operation with the supervisor tests setups to be carried out. The selection should aim at good comparison between results from test using the two different landslide blocks, porous and solid.

3. Study the existing model set-up and the installed instrument. Carry out a model test to study the overtopping of embankment dam from landslide generated waves.

   A wave will be generated using a porous slide and the corresponding wave height, overtopping volume and overtopping depth above the dam crest in the model will be monitored and studied. The speed of the slide will be varied by adjusting initial location of the slides. A dam with an upstream slope of 1:1.5 will be used in the experiments Freeboard will be in accordance with Norwegian regulations for dam consequence class 3 and 4 (f = 6 m and 4,5 m respectively).

   For the porous slides: The experimental results will be used to study the following:
   - The impulse wave generation and propagation.
   - Relation between the landslide and overtopping depth,
   - Relation between the landslide and dam overtopping volume,
   - Impact of landslide velocity on the overtopping volume.

4. Perform analysis of the data and study the effect of the different parameters. Compare results from test using the two different landslide blocks, porous and solid (solid from previous studies).

5. Complement results from previous studies using the solid block.

6. Conclusions and proposal for future work

NTNU

3 Supervision

Associate Professor Fjóla G. Sigtryggsdóttir will be the supervisor and provide guidance on the process of the study. PhD candidate Netsanet Nigatu will be a co-supervisor.

Discussion with, and input from colleagues and other researchers or engineering staff at NTNU, SINTEF, power companies or consultants is highly recommended. Significant inputs from others shall, however, be referenced to in a convenient manner.

The research and engineering work carried out by the candidate in connection with this thesis shall remain within an educational context. The candidate and the supervisors are free to introduce assumptions and limitations which may be considered unrealistic or inappropriate in a contract research or a professional/commercial context.

4 Report format and submission

The report should be written with a text editing software. Figures, tables and photos shall be of high quality. The report format shall be in the style of scientific reports and must contain a summary, a table of content, and a list of references and information about other relevant sources.

The report shall be submitted electronically in Inspera Assessment (IA) along with a summary. The summary shall not exceed 450 words. Supplementary working files such as spreadsheets, numerical models, program scripts, figures and pictures shall be uploaded to Inspera Assessment (IA) as applies or submitted to the supervisor.

The candidate shall present the work at an MSc seminar. The presentation shall be given with the use of powerpoint or similar presentation tools. The data and format for the MSc. seminar will be announced during the semester.

Trondheim, February 2019

Fjóla Guðrún Sigtryggsdóttir
Associate Professor
Department of Civil and Environmental Engineering, NTNU

Abstract

A landslide falling into a reservoir transfers its kinetic energy to wave energy. This wave energy generates an impulse wave that propagates away from the impact zone of the landslide. The generated impulse wave may cause damage as it runs up the shores or against the dam structure. Such large waves may cause hazardous consequences to the downstream area of the reservoir. Such is the case in the Vajont dam failure of 1963 in Italy, which was the cause of the loss of more than 2000 people.

The work in this thesis is an experimental study performed on a conceptual physical model with a scale of 1:190. The physical model simulates a real situation of a landslide into a reservoir and the possible consequences of this landslide. The main objective of this study is to investigate dam overtopping due to waves induced by a landslide into a reservoir and compare the presented experimental results of using porous blocks and solid blocks. For this experimental study, 123 laboratory tests were carried out.

A comparison of the experimental result of using a porous block to a solid block has been performed. For both solid and porous blocks, a similar wave pattern was observed. The generated wave amplitude ratio ($a_{\text{solid block}}/a_{\text{porous block}}$) was in the range of 0.88 to 1.67. The impact of different model parameters and slide properties on the overtopping volume, on the maximum overtopping depth, and on the wave generated is studied. The generated wave height is greatly dependent on the release height, weight, and porosity of the block. The release height, weight, and porosity of the block have an impact on both the overtopping volume and the maximum overtopping depth over the dam crest. The comparison result of the porous and solid block was compared to the literature results, and quite similar results were observed to Heller and Spinneken, (2013) and Ataie-Ashtiani and Nik-Khah, (2008). Additionally, the actual overtopping volume and overtopping depth along the dam crest are compared to the overtopping volume and maximum overtopping depth calculated by Kobel et al. (2017). Kobel et al. (2017) overestimate the overtopping volume; the ratio of $V_{Kobel}/V_{measured}$ falls in the range of 1.46 to 2.7. But close results are observed for the maximum overtopping depth over the dam crest except for few results.

Acknowledgment

First and for most, I would like to thank the 'Almighty God' for giving me healthy, strength, knowledge, ability, and opportunity to undertake, persevere and complete this work.

I gratefully acknowledge the Norwegian Agency for Development Cooperation's (NORAD) for providing me a full scholarship opportunity to study the master's program in Hydropower Development at the Norwegian University of Science and Technology (NTNU).

I would like to express my deep and sincere gratitude to my main supervisor Prof. Fjola Gudrun Sigtryggsdottir; for being always helpful, supportive, critical comments and invaluable guidance throughout this thesis work. Prof. Fjola always gave time for my thesis work, and her door was open whenever I had a question and needed help on my research. It was a great privilege and honor to have a supervisor like her.

Beside my main supervisor, I would like to thank my co-supervisor Netsanet Nigatu (Ph.D.) for her valuable comment on my thesis work and continues support, advice, and guidance throughout my laboratory work. It might be difficult to complete this thesis work without her support.

Special thanks should also be given to Eng. Geir Tesaker; who gave me technical guidance in the laboratory work and prepared me the required material for the laboratory work, and also NTNU staff who gave me academic knowledge and practical skills throughout my study.

Finally, many thanks to my family and friends for supporting me throughout my life.

Table of Contents

List of Figures

List of Tables

Abbreviation

a – Wave amplitude
a_M – Maximum wave amplitude
c – Wave celerity
CH – Wave channel
$c1, c2 \ldots c5$ – Crest 1, Crest 2 … Crest 5
do – Maximum overtopping depth
ds – Change in distance
dt – Change in time
E – Maximum wave overtopping depth parameter
g – Gravitational acceleration
h - Still water depth
H – Wave height
kg – Kilogram
L – Wavelength
l – Liter
m – Meter
mm – Millimeter
m^3 – Cubic meter
$NTNU$ – Norwegian University of Science and Technology
NVE – Norwegian water resource and energy directorate
Q – Discharge
Sec – second
T – wave periods
t – time
U/s – Upstream
V – Volume
Vs – Slide impact velocity
w – Dam height
ΔZse – Height of center of gravity
$1B$ – One block
$2H$ – Two blocks in horizontal arrangement
$2V$ – two blocks in vertical arrangement
$4B$ – For block arrangement
ɑ – Slide impact angle
β – Upstream dam face angle
σ – Dynamic bed friction angle
ε – Relative wave amplitude

1 Introduction

1.1 Background

Reservoirs are often built to store water for different purposes. Especially in mountainous areas, reservoirs are often built for hydropower production. Different problems are observed in the construction of reservoirs. Among these problems is the potential problem of landslides.

Landslides are one of the components in the erosion process, which has been described as a continual leveling of the surface features of the earth (Gaurina-Medjimurec, 2015). There are different principal drivers of the landslide phenomena. Precipitation, earthquakes, and volcanic eruptions are the natural drivers of landslides; while disturbance of the hillside due to human activity for different purposes is considered as an artificial driver. Both natural and human-made activities are the main reasons for landslide occurrence (Gaurina-Medjimurec, 2015). The landslide materials are subdivided into either a high-density material or a low-density material. The mass flows which consist mainly of rockfall material and granular soil material are considered as a high-density material; while glacier fall and snow avalanches are low-density materials (Fritz and Hager, 2003).

A landslide into a reservoir is one of the causes for dam failure. Dam failure is an uncontrolled flow of water out of the reservoir through a dam structure. Most often dams are constructed in narrow valleys. Due to the reservoir filling, the saturation level of the area is changed; which increases the possibility of the occurrence of a landslide. The landslide hazard from the bank of the reservoir is a potential threat to the dam structure and the downstream area of the dam. Across the world, many reservoirs are susceptible to landslides with a potential risk of overtopping due to waves generated by the landslide (Gohari and Avarideh, 2018).

Based on the landslide's position relative to the still water level, these landslides may be divided into three categories: sub-aerial landslides, partially submerged landslides, and submarine landslides (fully submerged). Figure 1-1 shows the three position of landslide into reservoir relative to the still water level. The initial position of the landslide determines the physical characteristics of the process, particularly the effect of the air on the landslide process. For sub-aerial landslide impacts, there are three important phases: the still water level, the slide material, and the effect of the air. The submarine landslide is treated as a two-phase flow, consisting of slide material and water interaction (Fritz and Hager, 2003).

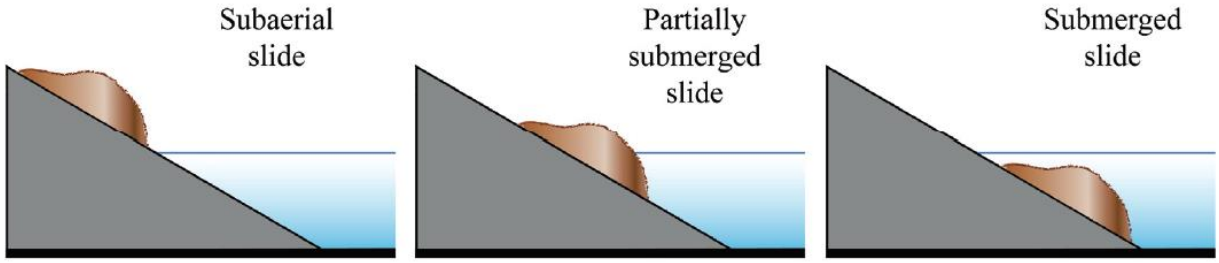

Figure 1-1 The position of landslide to reservoir relative to still water level (Heller et al., 2009)

A landslide falling into a water body generates impulsive water waves that are usually referred to as a category of tsunami waves (Ataie-Ashtiani and Nik-Khah, 2008). The generated impulse waves may cause damage as they run up the shores, or against the dam retaining a reservoir. Such large such waves may overtop dams with a hazardous consequence in the downstream area. The hazard may be intensified in the case of an embankment dam. It may cause complete failure of a dam during such an extreme loading condition.

The Norwegian water resource and energy directorate (NVE) in collaboration with NTNU initiated a research program on the impacts of landslide-generated wave action on embankment dams, particularly on rockfill dams. For this, experimental work has been carried out on a physical model in the Hydraulic Laboratory at NTNU. In 2014, an experimental test was carried out with different landslide scenarios and dam parameters. The physical process and interaction between the landslide-generated waves and dam overtopping were studied. A comparison was also made between the results obtained from the experimental test with the result from the computational method recommended by Heller et al, (2009). In the year 2015 and in the spring of 2016 experimental tests mainly focused on slide volume and dam characteristics were performed under several different scenarios, by varying the slide volume, the reservoir water level, the upstream dam face slope, and the upstream dam face roughness. During the fall period of 2016, 2017, and 2018 a study continued to check the effect of different parameters on the wave created and on the amount of overtopped water. Additionally, the sliding ramp was moved to the other side of the reservoir to investigate the potential laboratory effects on the previous set-up.

The above-mentioned studies enhanced the understanding of the effect of different dam parameters on the generated waves and overtopped water. Most of the above studies were carried out with a solid block material (no porosity). In this study, porous landslide blocks are used. In a real situation, especially in mountainous terrain, different landslide types can occur, e.g. earth slide and rockslide. The porous landslide blocks aim to simulate the earth slide material; whereas the solid blocks are to simulate the rockslides.

1.2 Objective

The main objective of this thesis is to use the physical model to investigate dam overtopping due to waves generated by a landslide into a reservoir and compare the experimental result of porous blocks and solid blocks. This investigation is mainly conducted using a porous block landslide, but experimental tests have also been carried out using solid blocks. The main focus of using two types of blocks is to compare the result and study the effect of the porosity of the material.

1.2.1 Specific Objective

A wave was generated using porous landslide blocks, the corresponding characteristics of the generated wave, the maximum wave height, the overtopping water volume and the maximum overtopping depth along the dam crest was monitored and studied. The experimental result is used to study the following:

a. The landslide impulse and pattern of wave generation and propagation
b. The landslide impulse and the generated wave height in the reservoir
c. The slide impulse and dam overtopping volume of the water
d. The slide impulse and the maximum overtopping depth above the dam crest and
e. Overtopping discharge along the dam crest

1.3 Stractural Layout of the Thesis

This thesis is presented in seven chapter and appendix. The contents covered in each chapter is described as follows.

Chapter one: This chapter presents the general background of this thesis and general information about landslides and landslide generated waves. The objective and layout of the thesis is described in this chapter.

Chapter two: This chapter describes general historical information about landslides around the world and the case of the landslides in Ethiopia. The impulse wave theory and the different types of waves are discussed. Additionally, some research work on the wave generated by sub-aerial landslides is considered in this section. Generally, this is the literature review of this study.

Chapter three: In this chapter a general introduction of the physical model is presented. The main part of the model and some instruments installed on the model are discussed in this section. Additionally, the sliding block properties and the calibration of some of some sensors are explained.

Chapter four: In chapter four, the previous studies performed on the physical model are discussed; along with the research gaps.

Chapter five: The total list of the tests performed in this study and the list of the tests performed by other students are given in this chapter. The general test procedure followed in the lab during each test is described in this part.

Chapter six: In this chapter the test results are analyzed and discussed. The wave generation and propagation are considered here. The impact of different model parameters and the sliding blocks' properties on the overtopping volume of water are analyzed. A comparison of test results for the porous and solid blocks is performed in this chapter. Additionally, a comparison of the test results against the literature is presented.

Chapter seven: This chapter gives the conclusion and recommendations for future studies.

2 Literature Review

2.1 Landslide and Landslide Generated Wave.

Landslides are one of the most prevalent geohazards, often bearing the characteristics of a natural disaster. Nearly 9% of natural disasters in the world is related to landslides (Skrzypczak et al., 2017). Many worldwide known landslides have been activated from prehistoric to recent times; they are remarkable due to their huge volume and the enormous damage they create. Table 2-1 shows the most known and deadly landslides from the prehistoric to recent time periods (Gaurina-Medjimurec, 2015).

Table 2-1 The most known and hazardous landslides from historical periods to recent periods (Gaurina-Medjimurec, 2015)

Landslide	Country	(Re)Activation Time (year)	Landslide Type	Landslide Volume (m^3)	Causalities
Storegga Slide	Norway	8,000 years before	Submarine landslide	840,000,000	-
Goldau	Switzerland	1806	Debris avalanche	40,000,000	457
Frank Slide	Alberta, Canada	1903	Rockfall	91,000,000	-
Kansu	China	1920	Debris flows	-	180,000
Khait	Tadzhikistan, (former USSR)	1949	Debris avalanches	-	12,000
Vaiont	Italy	1963	Rockslide	260,000,000	2,000
Vargas	Venezuela	1999	Debris flow	1,600,000	10,000
Leyte	Philippines	2006	Mudslide	-	1,120
Oso	USA	2014	Mudslide	10,000,000	41
Badakhshan	Afghanistan	2014	Mudslide	-	1,500

A landslide falling into a water body with a huge impact to the water's surface creates a landslide tsunami. This water wave creates hazardous consequences to the coastal areas, lakes, dams and also to far downstream areas of a reservoir (Take and Mulligan, 2017). The potential damage from such landslide events is created over time. One such catastrophic phenomenon is the Vajont landslide disaster in 1963 (Rinaldo and Monica, 2005). The Vajont dam is a double curvature arch dam of 276 m height. It was constructed during the period of 1957 to 1960 on the Vajont river. A slide mass with a volume of approximately 270 million cubic meters of landslide collapsed into the reservoir within less than 45 seconds. The landslide generated a wave which had a height of 140 m above the dam crest. The generated wave hit the town of Longaron and another village. Due to this catastrophe around 2000 people lost their life (Rinaldo and Monica, 2005). Figure 2-1 shows the situation of Vajont before and after failure.

Figure 2-1 Vajont reservoir before failure and after failure respectively (Landslides Mudslides, 2008)

2.2 Landslides in Ethiopia

Landslide hazards are one of the crucial environmental problems for the development of Ethiopia. This problem is one of the limiting factors for its urbanization and infrastructure projects. Specifically, for all activity performed on and at the foot of the slopes, landslides are major problems. There have been different levels of damage due to landslides at different times. From the year 1993 to 1998, due to landslides, more than 200 houses were destroyed, more than 500 km of roads were damaged and about 300 people were killed (Abebe et al., 2010). In Ethiopia, the major landslides are triggered by rainfall. The sliding materials include debris (earth slide or earth flows), and rock slides (Woldearegay, 2013). Figure 2-2 below shows a rockslide and associated earth slide on volcanic terrain in the central highland of Ethiopia, and damaged roads in the Blue Nile basin due to a landslide.

Figure 2-2 (a) Large-scale rockslide and associated debris/earth slides/flows on volcanic terrains, Tarmaber area, central highlands of Ethiopia. (Woldearegay, 2013); (b) a road section damaged in August 1993; (c) Damaged bridge due to landslide in the Blue Nile basin (Ayalew, 1999).

Regarding the construction of large dams, Ethiopia has different environmental problems. Landslides are one of the major factors that create problems for the construction of large dams. The Tekeze reservoir is one of the hydropower sources in the northern part of Ethiopia which was affected due to a landslide. In April 2008 a massive landslide occurred near the dam site. The landslide forced the developer to pay for additional costs for a retaining wall to keep back the eroding slopes (Tekeze Dam, Ethiopia, 2008.). Additionally, a slope stability problem was reported on the reservoir side of the Tekeze hydropower project. In addition to Tekeze, Gilgel Gibe hydropower is the main source of power production in Ethiopia. The catchment of the Gilgel Gibe I reservoir is located in the south west of Ethiopia. This is one of the regions in Ethiopia that was heavily affected by landslides. These landslides cause social, economic, and geomorphological problems. One

of the problems is the filling up of the Gilgel Gibe reservoir with sediments. Figure 2-3 shows the landslide which occurred in the upper part of the Gibe catchment. It is a small landslide which occurred on August 24, 2009 (Broothaerts et al., 2012).

Figure 2-3 Example of shallow landslide in the Gilgal Gibe catchment. Landslide area is 700 m2, volume 1400 m3 (August 24, 2009) (Broothaerts et al., 2012).

2.3 Impulse Wave Theory

Impulse waves typically occur in the open ocean, bays, lakes, and reservoirs. There are a different situations that cause an impulse wave; landslides, rockfalls, shear instability, avalanches or glacier calving, and wind are the main reasons (Heller et al., 2009). In extreme cases the wave created results in the overtopping of the dam with a catastrophic consequence and damage to the infrastructures (Evers and Hager, 2015). Alpine regions face a high risk of such events in view of their steep valley flanks, their potentially large slide volume and with high impact velocities. As shown in Figure 1-1 impulse waves are generated in three ways due to the landslide position relative to the still water level. The generated wave has three phases: wave generation, wave propagation, and wave run-up or dam overtopping (Heller et al., 2009). Figure 2-4 shows the three phases of the impulse wave generated. In each phase, the wave has its own properties.

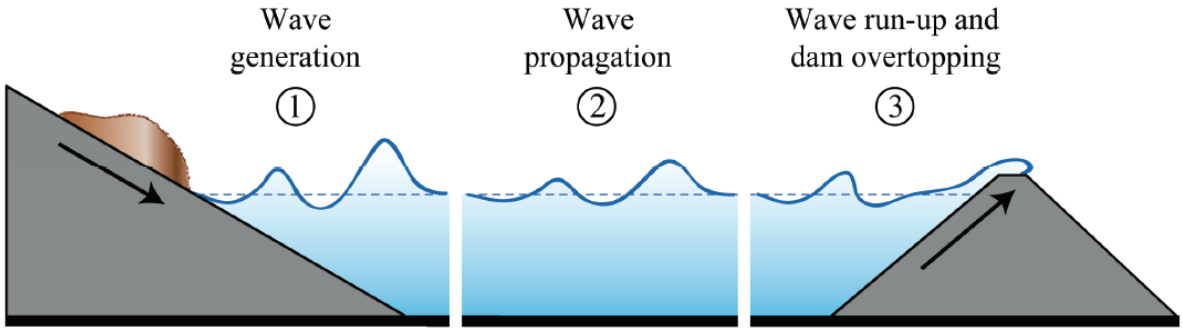

Figure 2-4 The three phases of the impulse wave generated, from wave generation to overtopping (Heller et al., 2009)

Water waves are like sinusoidal waves. Theoretically, water waves are different from the ideal sinusoidal wave. The wave created due to a landslide is a non-linear wave; while sinusoidal waves are linear waves. The wave type generated by a landslide may be allocated to one of the following four wave groups (Heller et al., 2009):

1. Stokes wave
2. Cnoidal wave
3. Solitary wave and
4. Bore wave

2.3.1 Stokes Wave

Stokes waves are steeper than sinusoidal wave types; where the wave trough is flatter and longer compared to the wave peak. It is a deep water or intermediate water wave. In Stokes waves the length of the crest and the trough is similarly long and also at least two similar crests can be observed (Heller and Spinneken, 2015). The wave type generated by wind is taken as an example of a Stokes wave. In Stokes waves slight flood mass transport takes place (Heller et al., 2009). Figure 2-5 below shows the stokes wave profile.

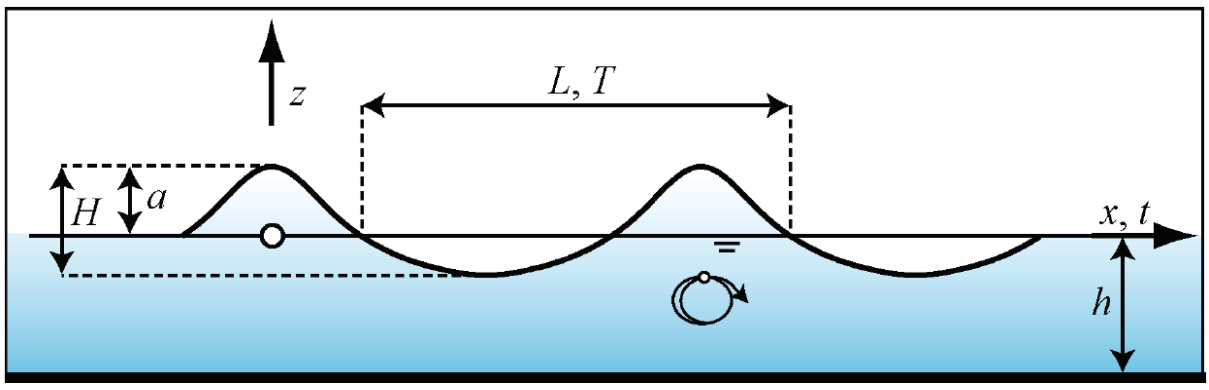

Figure 2-5 Stokes wave type profile, including the main wave parameters; in this wave type there is less fluid mass transport (Heller et al., 2009)

2.3.2 Cnoidal Wave

A cnoidal wave is a periodic wave in intermediate or shallow water depth. A wind generated wave in shallow water is considered as a cnoidal wave type. The cnoidal wave has mainly an oscillatory character, but also exhibits open water particle orbits and hence transport of fluid mass (Heller et al., 2009). Figure 2-6 show the cnoidal wave type profile; in cnoidal waves both the trough and the crest have a similar manner; the trough is more pronounced than the crest (Heller and Spinneken, 2015).

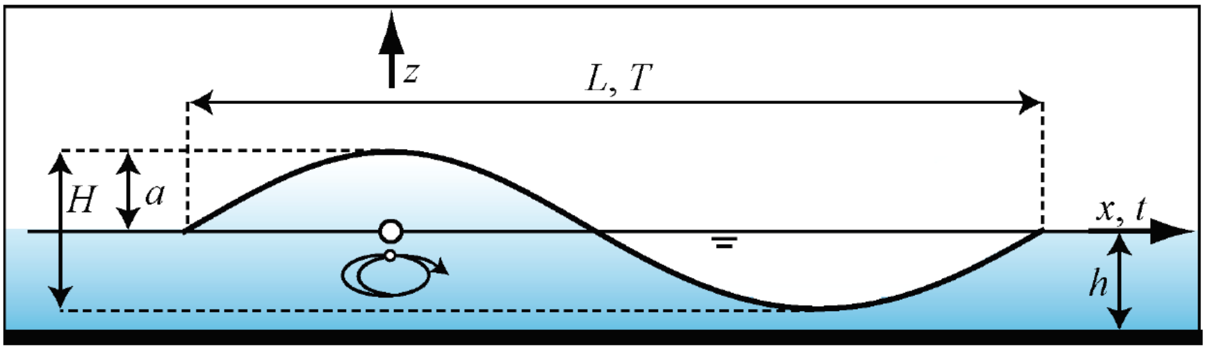

Figure 2-6 Cnoidal wave type profile with the main wave parameters; in this type of wave there is slight transport of fluid mass (Heller et al., 2009)

2.3.3 Solitary Wave

A solitary wave is a non-linear shallow water wave ($L/h > 20$). It is a classic tsunami, usually caused by the movement of tectonic plates. It has no wave trough and only consists of a wave peak as shown in Figure 2-7. In the case of this wave type, wave amplitude and wave height are similar (*a=H)*, although the wavelength is infinity ($L = \infty$). On a horizontal bed of a rectangular channel, in theory, this type of wave can propagate for unlimited distances without changing wave state. But in reality, turbulence may result, in which case the wave height decreases. The wave celerity is calculated by the following equation (Heller et al., 2009):

$$C = \left[\frac{g}{h+a}\right]^{1/2} \quad \ldots\ldots\ldots\ldots\ldots\ldots\ldots\ldots\ldots\ldots 2\text{-}1$$

Where

- $a \ldots\ldots\ldots\ldots wave\ amplitude$
- $c \ldots\ldots\ldots\ldots wave\ celerity$
- $g \ldots\ldots\ldots\ldots gravitational\ acceleration$
- $h \ldots\ldots\ldots\ldots still\ water\ depth$

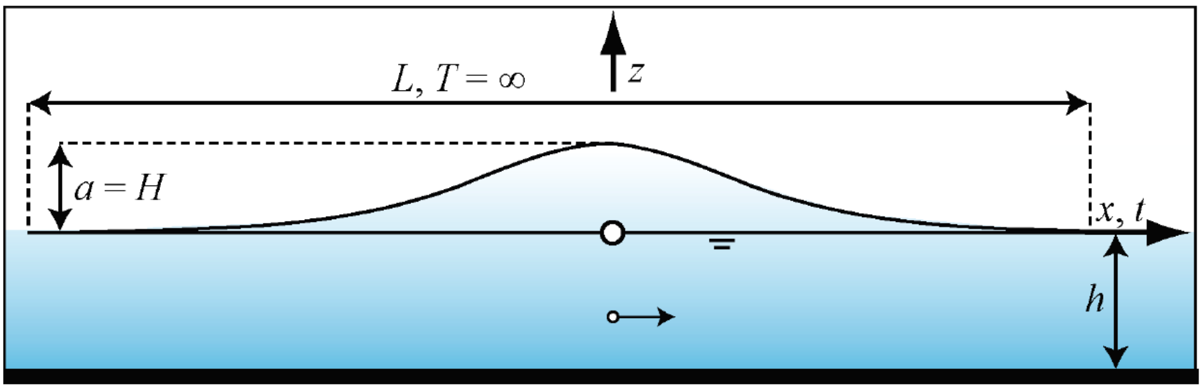

Figure 2-7 Solitary wave type profile; the profile shows the wave parameters and transport of fluid mass (Heller et al., 2009)

2.3.4 Bore Wave

A bore wave is a shallow water wave created when a wave breaks near the shore or when the wave crest is curled over by air. In a Bore wave, particles of water move horizontally

with large fluid masses. As show in Figure 2-8 the wave profile has a steep slope in front, with a gentle slope from the back.

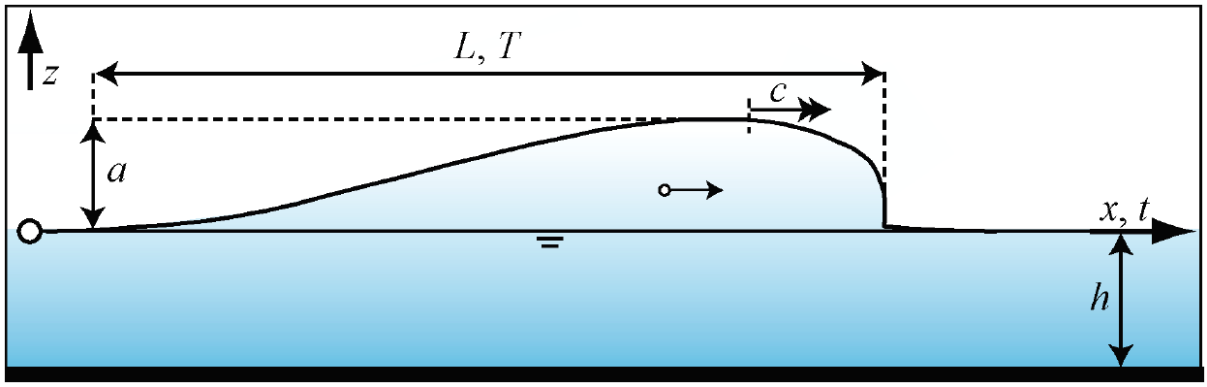

Figure 2-8 Wave profile of a bore wave with the most important wave parameters; large fluid mass transport (Heller et al., 2009)

2.4 Wave Generation and Propagation

A wave is generated in different ways. Specifically, for a reservoir wave it is generated due to external force applied to the water. A wave is generated in a natural or human-made reservoir due to a landslide (Heller et al., 2009). When the landslide falls into the body of water, it transfers its kinetic energy to it. This energy transfer displaces the water primarily in the direction of the landslide's motion. Due to this displacement of water a radial wave is generated that propagates away from the impact zone (McFall and Fritz, 2016). The way in which the generated wave travels is called wave propagation. In the case of landslides into a reservoir Heller et al. (2009) have identified two extreme cases in which the landslide mass impacts the reservoir.

- The first case is where slide material impacts longitudinally into a long reservoir; dimensionally the width of the slide material is either greater or equal to the reservoir width. The generated impulse waves are confined as they propagate along the reservoir and are not able to propagate laterally. The wave propagates in the direction of the landslide movement. It is illustrated in Figure 2-9 as case 1.
- In case 2 the slide material impacts at some location of the reservoir and additionally the width of the slide material is less than the width of the reservoir, at the contact area of the reservoir. In this case the generated wave freely propagates radially (Heller et al., 2009).

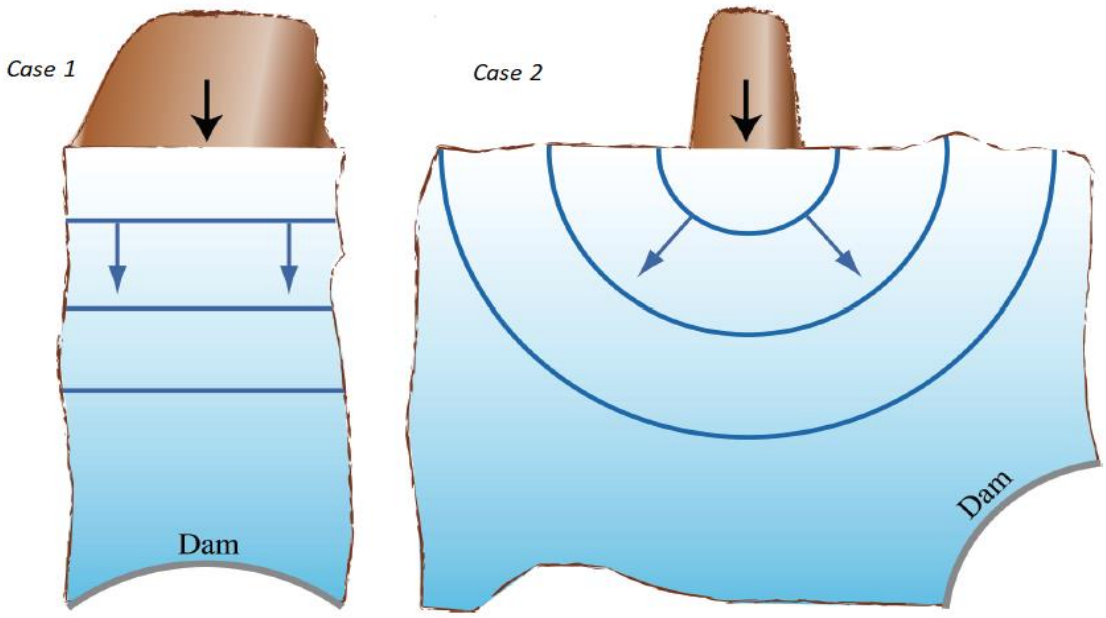

Figure 2-9 Reservoir geometry for two idealized extreme cases: case 1 for longitudinal slide impact with confined wave propagation; and case 2, wave propagation is radially from the impact zone (Heller et al., 2009).

In the above extreme case, the wave height changes rapidly in case 2 since the wave energy propagates over a large area. The geometrical similarity of the model and the prototype must exist to extrapolate the result from the model. There is a different parameter that influences the calculation of the maximum wave amplitude and maximum wave height. The parameters listed below influence the calculation.

- Slide impact velocity
- Bulk slide volume
- Slide thickness
- Slide width or reservoir width
- Bulk slide density
- Bulk slide porosity
- Slide impact angle
- Still water depth

2.5 Impulse Wave Generated by Sub-aerial Landslide

Ataie-Ashtiani and Nik-Khah, (2008) has been studied an experimental investigation on impulse waves caused by sub-aerial landslides. The experiment was carried out in a *2.5-m* wide, *1.8-m* deep, and *25-m* long wave tank, using a solid steel block and deformable granular materials as the sliding material. For the granular material, they tried using it confined in a very soft fabric and also, they used it naturally without any confining material. Figure 2-10 shows the condition of the generated wave for rigid, granular and confined granular materials. The rigid block generates a large amount of wave and the generated wave amplitude is higher than the wave amplitude generated by the granular materials. For the granular material, the generated wave is less compared to the solid blocks. The granular slide generates up to a *35%* smaller wave amplitude compared to the solid blocks. Also, it gave up to a *30%* larger wave period than the block slides. They compared the

generated wave pattern by both the solid block and granular materials. They concluded that the general wave pattern in all experiments was the same, except for the amplitude and period. The wave pattern was strongly affected by the bed slope angle, the landslide impact velocity, the slide thickness and deformability. The slide shape did not strongly affect the wave pattern (Ataie-Ashtiani and Nik-Khah, 2008)

An experimental study was conducted by Heller and Spinneken (2013) on the comparison of the waves generated by solid slide and granular slide materials. The base of the comparison for both the solid block and the granular slides was that the material has an identical dimensionless parameter (F, S, M, and α) and the comparison should take place at an identical location. As per their conclusion, the wave generated by a solid block has a larger, equal, and smaller wave compared to the granular materials. The maximum wave amplitude ratio ($a_{blocks}/a_{granular}$) fell in the range of *0.43 to 1.76*. The wave period was dependent on the time of the submerged landslide motion rather than the width and front shape of the slide materials (Heller and Spinneken, 2013).

A comparison of the wave generated by combined solid blocks and granular materials to a pure solid and granular landslide was performed by Tang et al., (2018). In their comparison the main similarity of the sliding material is the identical slide mass and release height. As per their conclusion, the impulse wave generated by combined landslide material is larger than the impulse wave induced by solid landslides. Also, the generated wave amplitude by combined material is much larger than the wave amplitude generated by granular material for a small hill slope angle (Tang et al., 2018).

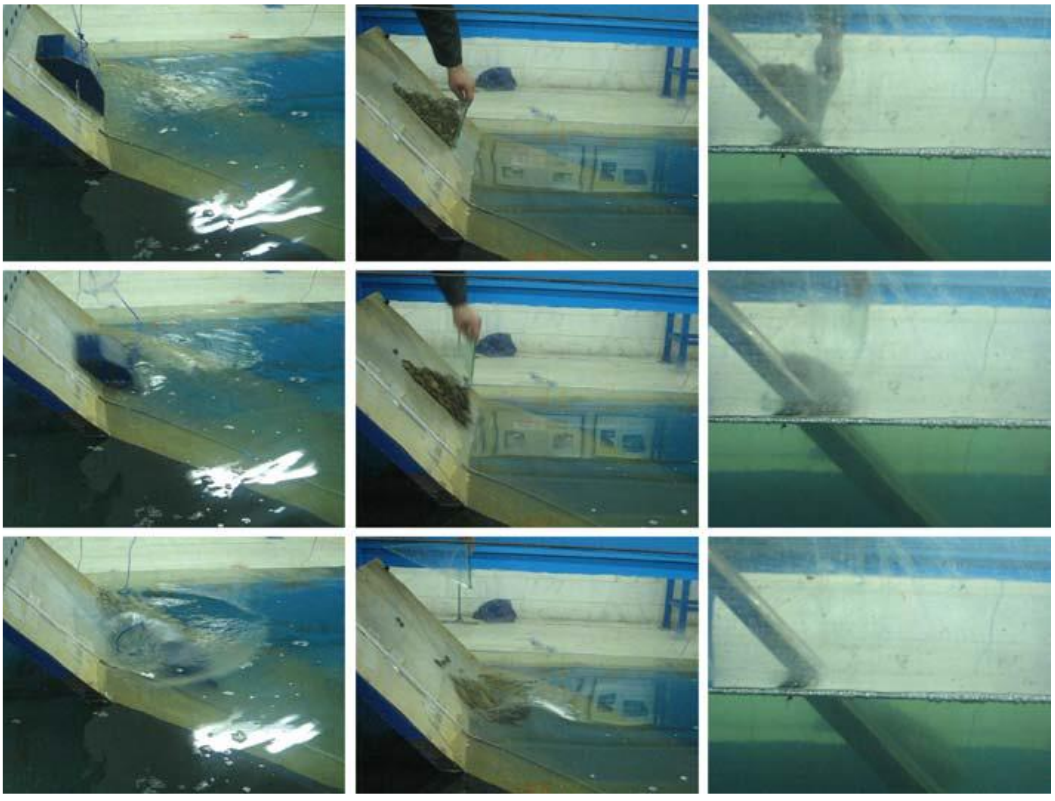

Figure 2-10 The condition of the wave generated based on the rigidity of the slide. From left to right: rigid, granular, and confined granular material (Ataie-Ashtiani and Nik-Khah, 2008)

3 Physical Model Description

A physical model is a simplified material representation (representation of the prototype), usually with a reduced scale of an object or phenomena that needs to be investigated. The geometry of the model and prototype are often similar; since the model is the rescaling representation of the prototype.

The physical model used in this study is a conceptual model; but a prototype scale of 1:190 has been considered. It was built about 10 years ago in the Norwegian University of Science and Technology, at the Department of Hydraulic and Civil Engineering. In the last decade, different research studies have been conducted on the model. Within the last few years, it has been modified to some degree depending on the research studies conducted on it. It simulates a landslide fall into a reservoir, generating a wave and the wave is propagated to the upstream face of the dam. It has different structural components; the main components being the reservoir, the dam, the landslide and the sensors. Figure 3-1 shows the plan view of the model. The buckets are labeled with numbers 1-5 and the subdivided dam crest is labeled with C1 – C5.

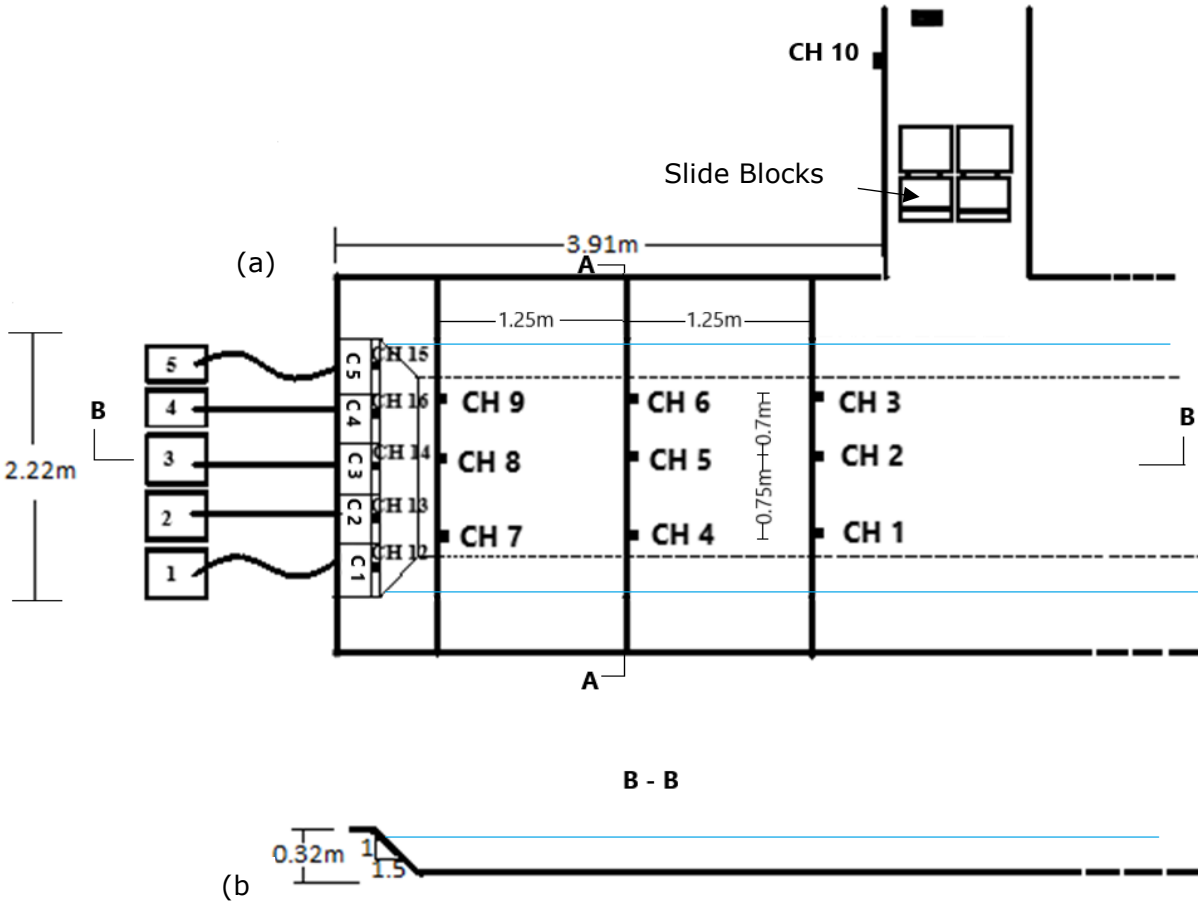

Figure 3-1 (a) Plan view of the physical model; (b) Cross-sectional view of the reservoir

A photograph of the physical model is presented in Figure 3-2. There are different instruments installed on the model. The names of some of the components are indicated on the photograph as shown below.

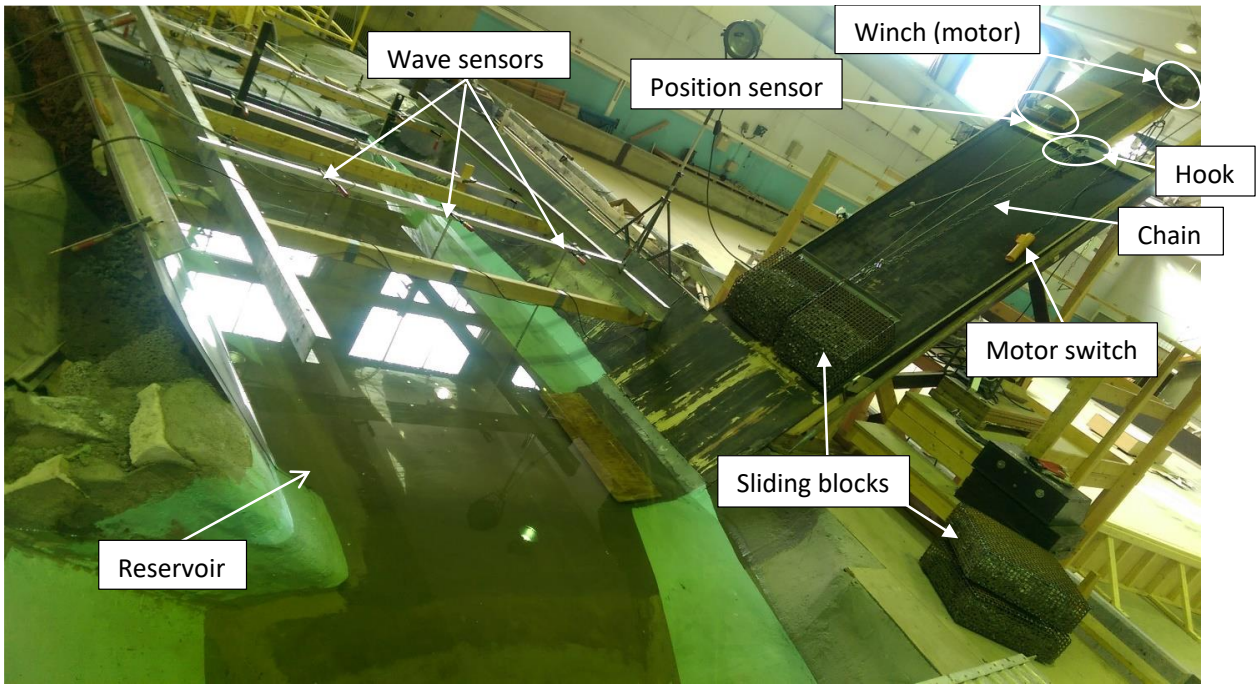

Figure 3-2 Photograph of the physical model

3.1 Reservoir

The reservoir has a trapezoidal shape. Each side of the reservoir bank is constructed from wood and it is plastered with a concrete cement mix. This concrete plastering helps the model to simulate the roughness of the sidewall to some degree. For the test performed on this physical model, the reservoir is filled to different water levels. The required depth of the reservoir is measured using a piezometer that has a level indicator inside the piezometer tube. The piezometer is adjusted to the required water depth and the water is filled from the normal waterline using a water pipe system. To decrease the reservoir level, the water is pumped out from the reservoir using a pumping system. Figure 3-3 (a) shows the reservoir of the physical model while Figure 3-3 (b) shows the piezometer that is used to control the level of water.

For this study, three different reservoir depths are considered. The depth of the reservoir is based on the Norwegian regulation for dam consequence class 3 (high hazard dams), class 4 (highest hazard dams) (Supervision of dams - NVE, 2015), and the minimum allowable depth of the reservoir.

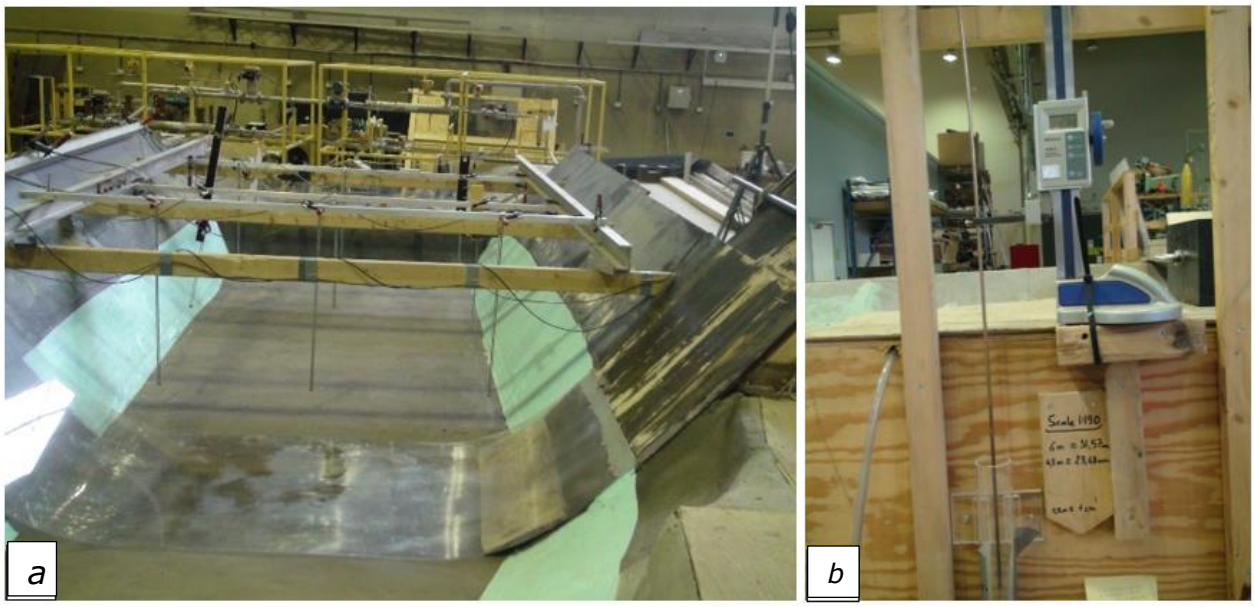

Figure 3-3 This figure shows (a) photograph of the reservoir and (b) photograph of the piezometer

3.2 Dam

The dam is one of the main components in this physical model. Dimensionally it has a height of *0.32 m* and a length of *2.22 m*, which represents an embankment dam. The upstream face of the dam is constructed from wood, so there is no structural damage during overtopping, rather than measuring the overtopping volume and the overtopping maximum wave created. The dam is easily removable, and replaceable with another type of dam with the same dimensions, but a different dam slope and surface finish. For this study the upstream face of the dam is constructed with a slope of *1:1.5* and it has a smooth surface finish. Figure 3-4 shows a photograph of the dam from the upstream side of the reservoir.

In this study three different freeboards of the dam are considered; the prototype freeboard of the dam follows the Norwegian regulation for dam consequence class *3* and class *4* (freeboards of *6 m* and *4.5 m* respectively) and the maximum allowable freeboard of *13 m* for this dam height. The model with the equivalent of the freeboard of the dam is *31.6 mm, 23.7 mm*, and *68.4 mm* respectively. The dam crest is subdivided into five parts. When overtopping occurs, the water flows up the dam crest in each subdivided part. The overtopped water is collected separately; this helps in the study of the overtopped water volume in different parts of the dam crest. Additionally, this division assists with the investigation of the maximum wave height along the dam crest length. Both the upstream dam slope and roughness affect the overtopping volume. In this study, since the dam slope and roughness are not changed for all test set-ups, its effect is not analyzed.

There are five buckets that collect the overtopping water during every test. The buckets are indicated in Figure 3-4. To measure the volume of water collected, calibration of the bucket is done before the start of the test. The calibration is shown in Appendix B.

Figure 3-4 Photograph of the dam from the upstream side and the overtopping water collecting buckets

3.3 Landslide and Sliding Plane

The sliding plane is constructed with a 50^0 inclination from the horizontal plane. It is made up of wood and has a smooth surface finish. There is a piece of plexiglass attached to the end of the sliding plane which goes through the reservoir and up to the opposite bank of the reservoir. The plexiglass helps the sliding material to move a long distance inside the reservoir and prevents the sliding material from stabbing into the bottom surface of the reservoir.

From the top of the sliding plane there is a winch and a position sensor (Figure 3-2 above). The winch is used to pull out the submerged blocks from the reservoir during the test process and also used to keep the block on the sliding plane. The position sensor is used to record the position of the block during sliding. The position sensor is connected to the computer and continuously records the position of sliding blocks in terms of voltage. To convert the voltage into distance, calibration is done for the position sensor. During each test, the position sensor is connected to the sliding block.

There is a slide trigger switch which is attached to the sliding blocks during every test procedure. The main purpose of the switch is to trigger every sensor of the model. The mode of recording is adjusted in the software by changing the triggering source to external analog. Every sensor is triggered by this triggering switch and the sensor starts recording when the switch is in the open position. The switch is closed by the sliding blocks, and as the sliding block starts to move the switch opens. At the same time, every sensor installed starts to record. Figure 3-5 shows the triggering switch connected to the sliding blocks and the connecting bar that is used to connect two blocks.

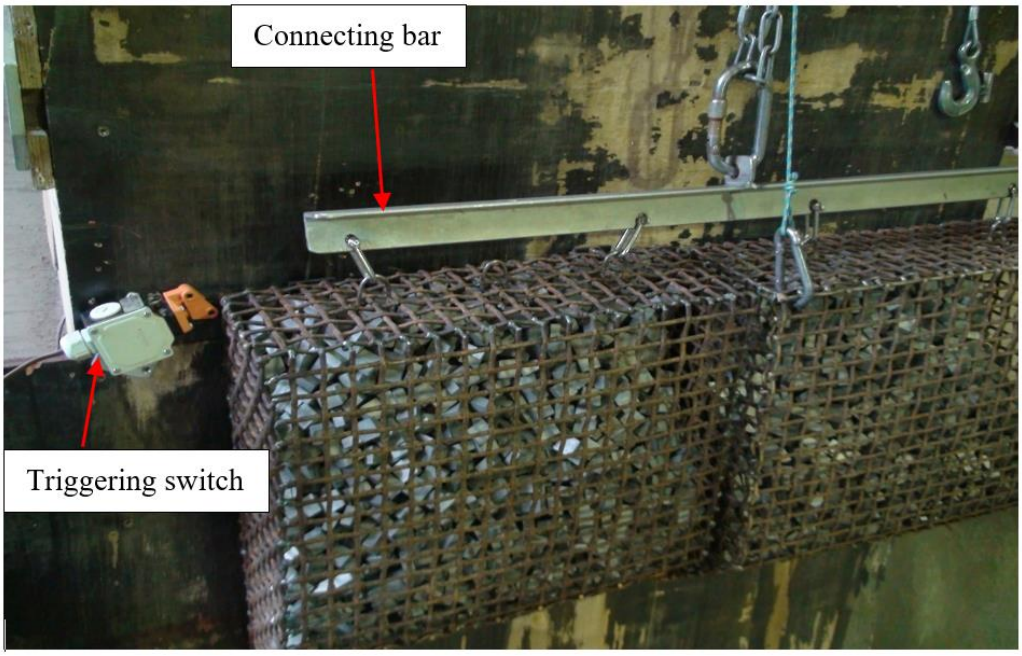

Figure 3-5 This figure shows the triggering switch connected to the landslide blocks and the bar connecting the block together

There are two types of landslide blocks for this test set-up. The first is the solid block slides, which simulate rock material, and the second, a porous block slide which simulates partial granular materials. There are eight solid blocks of different sizes, mass and density. There are two front blocks for both types of the blocks. The front blocks have a 45^0-bevel shape from the front side. The blocks following the front block have a rectangular shape. For this test set-up a maximum of four blocks are used: two front blocks and two blocks following the front block. Every block has a clip that helps to attach one block to the other block. The blocks are held on the sliding plane by a quick release hook.

The porous sliding blocks are prepared from small pieces of aluminum. The pieces of the aluminum are confined with a rigid confining material. There are four blocks: two front blocks with a 45^0-bevel shape and the same weight; and the other two have a rectangular shape and a similar weight. The shape of the confining material has a similar dimension to the dimension of the solid blocks. In addition to the shape of the blocks, the weight of the porous blocks is similar to the weight of the solid blocks. Table 3-1 shows the weight of the porous blocks and solid blocks; while Figure 3-6 shows the sliding blocks hooked on the sliding plane.

Table 3-1 Total weight of different slide block configurations both for solid and porous blocks

Block arrangement	Mass (Kg)	
	Solid blocks	Porous blocks
1B	37.7	37.7
2H	75.3	75.3
2V	80.1	80.1
4B	160	160

Figure 3-6 (a) Porous sliding blocks kept on the sliding plane; (b) Solid sliding block on the sliding plane, both show a four-block arrangement

In real situations a landslide may occur from a different position in the reservoir level; it may even occur from the inside part of the reservoir. In this study, the impact of the release height on the overtopping water volume is studied by changing the position of the sliding blocks. The release height of the blocks in this experiment is varied from *0 m to 1.5* m from the surface of the water along the sliding plane with an interval of *0.5 m*.

3.4 Sensor

In this physical model different sensors are installed to record different parameters. There are wave sensors, ultrasonic sensors, and position sensors. The position sensor is a sensor that records the position of the sliding block along the sliding plane in terms of voltage. Both the wave sensor and the ultrasonic sensor are explained below.

3.4.1 Wave Height Sensor

There are nine wave height sensors installed in the reservoir at different locations. These sensors are highly sensitive to small movements of water. In Figure 3-1 above, the wave sensors are labeled with the names *CH1* to *CH9*. The recording of the sensor is actuated by the triggering switch shown in Figure 3-5 above. In every test the sensors are calibrated before the blocks are released to the reservoir. Since the recorded data is in terms of voltage, it is converted to height using conversion factors. The following steps show the procedure to calibrate the wave sensors.

- First the reservoir should be filled to the required water level. After filling the reservoir to the required level, the zero level is fixed by setting each wave channel to zero voltage. This is done by rotating the rotatable switch on the wavemeter.
- In the second step, using the rectangular shape of the known thickness still piece, the bar holding the sensor is uplifted by 50 mm and the corresponding channel voltage is fixed to -1 volt.
- Finally, the sensors return to their original position before the test startup.

All the wave sensors are connected to the wavemeter; whereas the wavemeter is connected to the computer through a connecting cable.

3.4.2 Ultrasonic Sensors

There are five ultrasonic sensors installed on the dam crest. As explained in section 3.2, the dam crest is divided into five parts. These sensors are installed in every part of the dam crest. They measure the overtopping water depth and record the data in terms of voltage. So, to convert the recorded voltage into depth, calibration is carried out. The calibration is done by inserting a known thickness of material under the sensors and removing it several times. The calibration factor is the average voltage difference between the reading of the sensor without the material and after the material is inserted under the sensors. The detailed calibration calculation is shown under Appendix B. Figure 3-7 shows the overtopping sensors with the corresponding division of the dam crest.

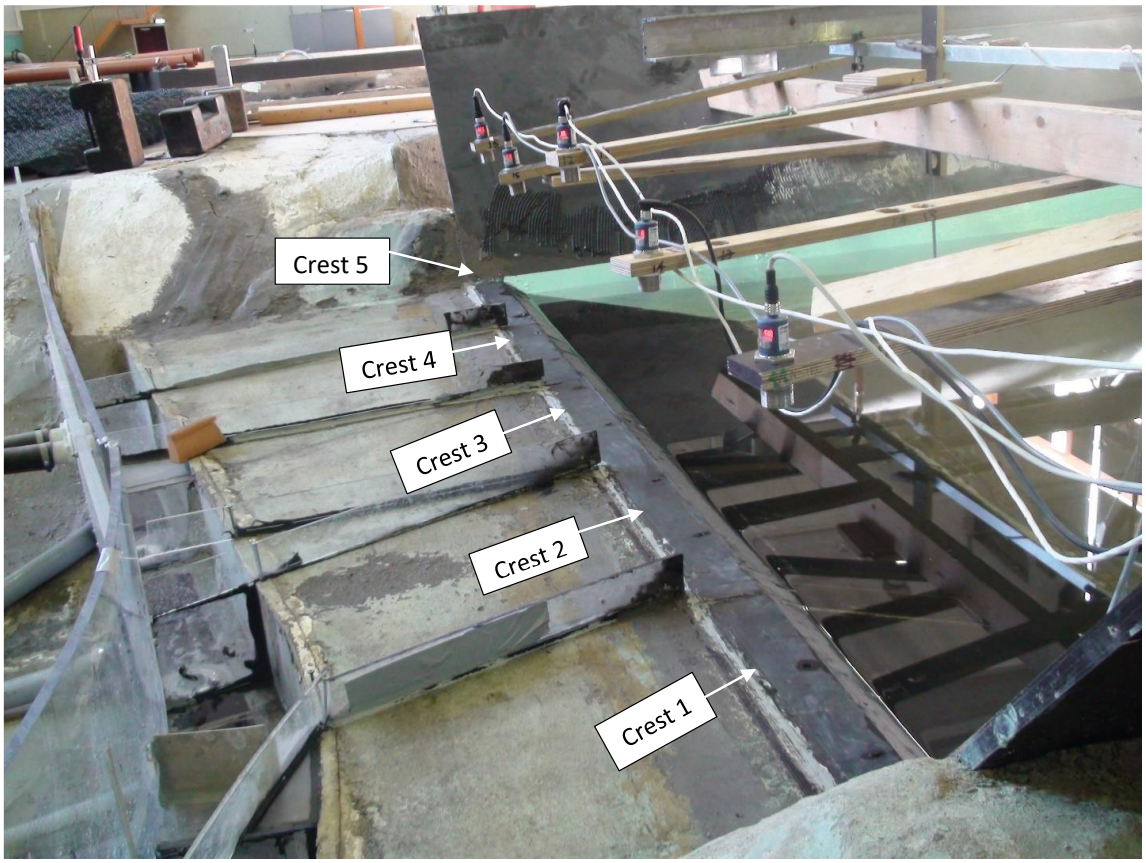

Figure 3-7 The five ultrasonic sensors used to measure the overtopped water depth on the dam crest and the corresponding subdivided dam crest

3.5 Computer, Wavemeter, and Digital Multimeter

The wavemeter is an instrument used to amplify the reading of the wave sensors. The nine wave height sensors are connected to the wave meter and calibration is done by rotating the rotary switch on the wave meter. There is a digital multimeter used to read the voltage of the wave meter during calibration of the wave sensors and position sensors. The

computer is installed with Agilent software. This software is used to read the sensor. Figure 3-8 shows the digital multimeter, wave meter and computer used for this test set-up.

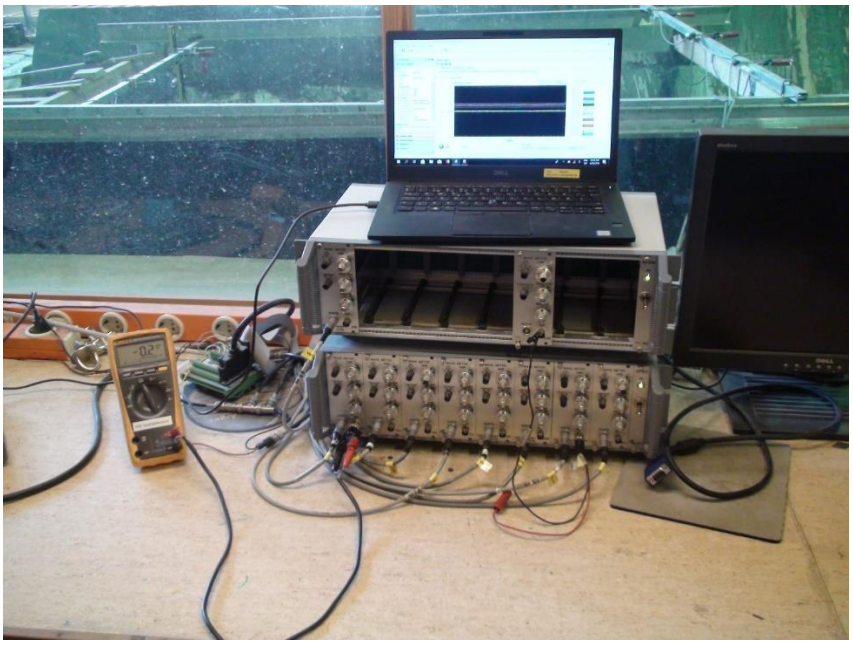

Figure 3-8 Photograph of the wave meter, digital multimeter, and the computer installed with Agilent software

4 Review of Previous Studies on the Model and Research Gaps

4.1 Previous Studies

The physical model used in this study was constructed about 10 years ago in the department of Hydraulic and Civil Engineering at NTNU. In the last decade, different research studies have been conducted with the model. The first research program was conducted between the collaboration of the Norwegian Water Resource and Energy Directorate (NVE) and NTNU on the impacts of landslide-generated wave action on embankment dams, particularly rockfill dams. After the completion of the research program, the model continued to be in use for different experimental studies. During 2014 different experimental tests were carried out in different landslide scenarios and with different dam parameters. The physical process and interaction between the landslide-generated waves and dam overtopping were studied. Using this model some research theses for the master's program were conducted over the last few years with different objectives.

In 2015 experimental studies were conducted by Bolzoni, (2015).The main aim of his study was to analyze the "Physical model study on the impact of landslide generated wave action on embankment dams." The thesis focuses particularly on the overtopping volume of water created due to landslide phenomena. Additionally, the result of the model test is compared with Heller's et al, (2009) numerical method. During his study, he considered different parameters and investigated their effect on the overtopping volume. The main parameters considered are landslide volume, upstream dam slope and roughness. Bolzoni, (2015) conducted around 17 tests by varying the slide volume, freeboard, and dam slope. Finally, he concluded that the run-up height and overtopping volume increased as the volume of the landslide increased. The change in dam roughness strongly affected the wave run-up height and the increase in freeboard decreased the overtopping volume. He also did a comparison with Heller's et al (2009) study and he concluded that the run-up height result from the physical model's test was underestimated 45-50% compared to Heller's et al. (2009) method. However, the overtopping volume was approximately 30-35% greater than in Heller's method (Bolzoni, 2015).

Two other master's students, Ponziani and Gardoni, (2016) done their final thesis using this physical model. The main objective of their studies was to undertake investigations on a scale model to gain knowledge about the impact of impulse waves generated by sub-aerial landslides on a rockfill dam. Around 130 experiments were performed to study the effect of the location and speed of the landslide movement on the wave generation, propagation and dam overtopping. In their studies they used different slide volumes, shapes, and fixed dam arrangements. Additionally, corresponding wave height, overtopping volume, and overtopping height were monitored in their studies. They rehabilitated the model to study the effect of the sliding plane position. Basically, there was a slide plane only on one side of the reservoir bank, but they introduced another sliding plane on the other side and compared the effect created due to the change in sliding position. They made a video recording to investigate the wave propagation and wave run-up height over the dam crest due to a landslide. In addition to the video they used MATLAB.

As per their conclusion, the slide impact velocity has no relevant influence on the wave propagation. However, they found that increasing the slide volume has an impact on wave propagation; as the slide volume increases the propagated wave height also increases. Parameters that have an impact on the overtopping volume of water were investigated in their studies. The slide volume is the most influencing parameter, although the shape of the slide and impact velocity have a big effect on the overtopping water volume. Finally, they suggested that further experimental investigation was required with different sliding plane structures; thus allowing the study of a wider range of the effect of impact velocity value, and further investigation with different dam types (Ponziani and Gardoni, 2016).

The most recent master's thesis using this physical model was conducted by Biedermann, (2017). The main objective of his thesis was to investigate the overtopping water volume, height, and discharge over the dam crest. In his study process, different parameters were considered, and it aimed to discover which parameter has a high impact on the overtopping water volume and on the distribution of overtopping water along the dam crest. He performed around *200* tests; among these tests, he accepted *135* of them as being reliable results for his work.

Biedermann, (2017) investigated the impact of the upstream dam face roughness on the overtopping height and overtopping volume of water. As per his conclusion, the variation of the overtopping water volume and overtopping height for smooth and rough dams vary less than *10%*. Taking the model's uncertainty into consideration (assumed as 10% uncertainty), the dam roughness couldn't have an effect on the overtopping height and water volume. The other parameter considered was the dam slope. Based on the result achieved he summarized that overtopping volume increases for mild slopes for the same slide volume and release height. Considering the effect of the freeboard, he performed several tests with two different freeboards and changed the volume of the slide as well. He concluded that the freeboard is the most influencing parameter for the overtopping water volume and can help to mitigate the effect of overtopping. The other parameter that has an effect on the overtopping volume is the landslide impact velocity and landslide volume. The impact velocity and landslide volume have a direct bearing on the amount of overtopping water volume (Biedermann, 2017).

During the period of 2017 and 2018 PhD candidate Netsanet Nigatu was using the model in her research.

4.2 Research Gaps

The main uncertainty, in a real landslide case, is mapping its geological behavior. It is difficult to predict the exact property of the landslide in a real situation. This is the case for the Vajoint dam failure, where the parametric properties of the landslide were underestimated (GENEVOIS, 2013). However, performing model tests for different parametric conditions and simulating different properties of the landslide may improve understanding of the landslide phenomena. The real topography of a reservoir area may not be of a regular shape. Most of the research studies are performed on regularly shaped reservoirs and regularly shaped landslide material. Most of the developed equation is also based on this regular shape and different parametric conditions; which may cause some uncertainty for real situations of landslide phenomena.

5 General Test Preparation and Performed Tests

In this chapter the general procedure followed to perform the test from the start to the end is presented. All the performed tests have the same general procedure, except the changing of some parameters according to the test instructions.

5.1 Test Preparation and Procedure

The first step of test preparation is adjusting the reservoir level to the required water depth. It is adjusted either by filling it if it is below the level or pumping out if it is above the level. The water level is controlled by the piezometer.

After the reservoir is filled to the required level, the release height of the block is measured from the level of the water to up the sliding plane; the sliding blocks are chosen as per the instruction of each test number and fixed to the appropriate release height.

- Once the sliding blocks are fixed to the required position, the triggering coil is attached to the sliding blocks and fixed to the sliding plane. The slide block keeps the triggering coil in a closed position; when the block starts sliding, it goes to an open position. At the same time the sensors start recording.
- To calibrate the position sensor, a measurement of the position sensor is taken from a known distance, by putting the measuring tape on the sliding plane. Then zero to the top position of the sliding plane and pull the position sensor rope to the known distance and record the corresponding voltage value. This value was used for the calibration of the position sensor. Once calibration is done the rope is connected to the sliding blocks.
- Prepare the buckets to collect the overtopping water. Before every test, the bucket level should be flattened and must have enough space to collect the overtopped water. Calibration of the bucket is done once for all tests.
- Put the camera stand in the selected position to record the video. The position is selected based on the requirement of the video.
- Open the computer and start the Agilent software. Check the proper functioning of the sensors on the display. If there is something wrong with the display adjust appropriately.
- Inspect overtopping sensors. There is a green light on the sensor that indicates that the sensor is in normal operating range. If the sensor is out of range the green light goes to red.
- If everything is working properly, press the record button on the Agilent software to start the sensors recording. Also start the camera to record the video and release the sliding blocks. The software records until overtopping stops.
- Finally, remove the blocks from the reservoir and the next test follows the same procedure.

5.2 Performed Tests in This Study

There are around 120 tests performed for both solid block material and the porous block materials. Tests in the parentheses are planned, but not performed, because the other

tests showed that there was no overtopping, only a small splash of water overflow. With similar parametric condition three tests are performed for each test. For the result analysis the average of the three test results are used. Table 5-1 and Table 5-2 show a list of tests for both solid and porous blocks respectively.

Table 5-1 List of performed test for solid blocks.

U/s dam Slope	Freeboard (mm)	Block arrangement	Release Height (m)	N° of test	Test number		
1:1.5	23.68	1B	1.5	3	287	288	289
			1	3	290	291	292
			0.5	3	293	294	295
			0	3	296	297	298
		4B	0	3	323/4.5	324/4.5	325/4.5
		2V	0	3	326/4.5	327/4.5	328/4.5
		2H	0	3	329/4.5	330/4.5	331/4.5
	31.57	1B	1.5	3	299	300	301
			1	3	302	303	304
			0.5	3	305	306	307
			0	3	308	309	310
		4B	0	3	323/6	324/6	325/6
		2V	0	3	326/6	327/6	(328/6)
		2H	0	3	329/6	330/6	331/6
	68.42	1B	0.5	3	311	312	(313)
		2H	0.5	3	314	315	316
		2V	0.5	3	317	318	319
		4B	0.5	3	320	321	322
		4B	0	3	332	333	334

- 23.68 mm represents for prototype of 4.5 m with a scale of 1:190
  31.57 mm represents for prototype of 6 m with a scale of 1:190
  68.42 mm represents for prototype of 13 m with a scale of 1:190

Table 5-2 List of performed tests for porous blocks.

U/s dam Slope	Freeboard (mm)	Block arrangement	Release Height (m)	N° of test	Test number		
	23.68	1B	1.5	3	335	336	337
			1	3	338	339	340
			0.5	3	341	342	343
			0	3	344	345	346
		4B	0.5	3	347	348	349
			0	3	350	351	352
		2V	0.5	3	353	354	355
			0	3	356	357	358
		2H	0.5	3	359	360	361
			0	3	362	363	364
		1B	1.5	3	365	366	367
			1	3	368	369	370
			0.5	3	371	372	373

1:1.5	31.57		0	3	374	375	376
		4B	0.5	3	377	378	379
			0	3	380	381	382
		2V	0.5	3	383	384	385
			0	3	386	387	388
		2H	0.5	3	389	390	(391)
			0	3	392	393	(394)
	68.42	1B	0.5	3	395	(396)	(397)
		2H	0.5	3	398	399	400
		2V	0.5	3	401	402	403
		4B	0.5	3	404	405	406

- 23.68 mm represents for prototype of 4.5 m with a scale of 1:190
  31.57 mm represents for prototype of 6 m with a scale of 1:190
  68.42 mm represents for prototype of 13 m with a scale of 1:190

5.3 Tests Performed by Other Students

For the comparison of the solid block result to the porous block result, tests for solid blocks performed by another student are used. Table 5-3 shows a list of tests used in this study from another student's data.

Table 5-3 List of tests used from another student

U/s dam Slope	Freeboard (mm)	Block arrangement	Release Height (m)	N° of test	Test number		
1:1.5	23.68	4B	0.5	3	61	62	63
		2V	0.5	3	52b	53	54
	31.57	4B	0.5	3	82	83	84
		2V	0.5	3	100b	101	102

- 23.68 mm represents for prototype of 4.5 m with a scale of 1:190
  31.57 mm represents for prototype of 6 m with a scale of 1:190

6 Result Analysis and Discussion

This chapter is mainly focused on the analysis of the test output. In the discussion, the effect of different parameters on the overtopping water is analyzed both for the porous blocks which simulate the granular material, and solid blocks which simulate the rock materials. Additionally, a comparison of the result for both solid and porous blocks is performed. For this comparison, some results are taken from previous tests performed by other students. All the analysis in this chapter is based on the model's parameters. For the prototype, the analysis result should be scaled with the Froude similarity. Since gravitation force is the dominant force, Froude similarity is applied.

6.1 Impulse Wave Generation and Propagation

When a sliding material falls down from elevated point the potential energy of the material will be transferred to kinetic energy. As the sliding material impacts the water's surface, it transfers its momentum to the water and due to that energy transfer, an impulse wave is generated (McFall and Fritz, 2016). In this study, different tests are performed, and the generated wave is dependent on different parameters. The situation when the sliding material hits the water surface is recorded and the result of the video is used for the subsequent discussion. When the sliding material hits the water's surface the water is pushed towards the opposite bank of the reservoir, towards the direction of the dam. The pushed water collides with the reservoir bank and is reflected in stoke-like waves. The generated wave with this form moves in the direction of the dam. When the wave height in front of the dam is greater than the freeboard of the dam overtopping will occur. Figure 6-1 shows when the sliding material impacts the water's surface and a wave is generated in different directions. In this figure, the situations for both porous and solid blocks are observed. As indicated in Figure 6-1 (a) and (b), when the wave is observed from the backside of the sliding material, it shows that the generated wave is moving in all directions. For the solid blocks, the diameter of the generated wave looks bigger than the wave generated by porous blocks. From the side view of the test set-up, when the sliding material touches the water's surface, it creates a splash of water in addition to the generated wave.

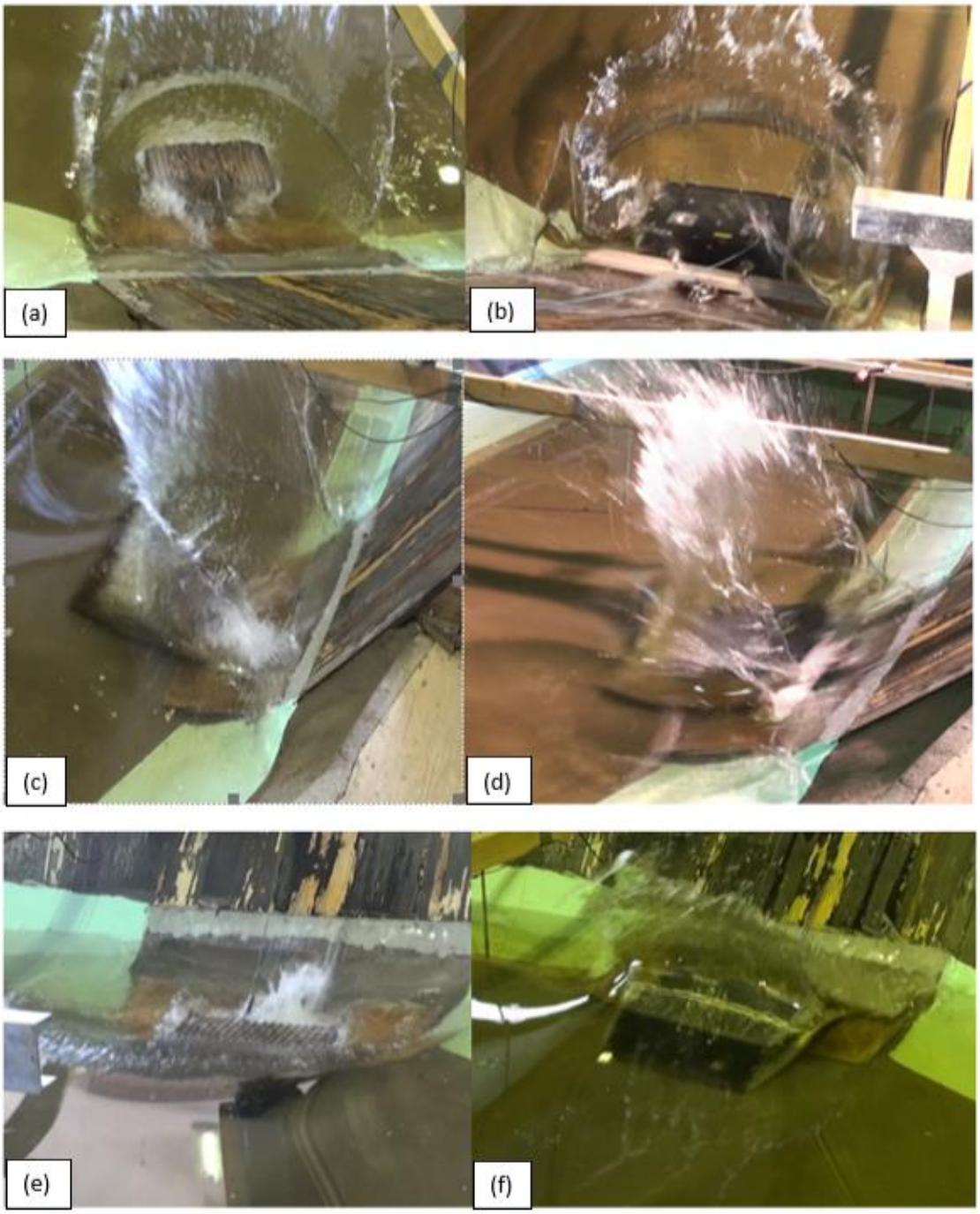

Figure 6-1 This figure shows the condition of the wave generation when the sliding materials fall into the reservoir. The block configuration and weight of the block are similar for both porous and solid blocks. All the figures on the right are solid blocks; while the figures on the left are porous blocks; (a) and (b) show the generated wave observed from the backward direction for both the porous and solid blocks respectively; (c) and (d) show when the set-up is observed from the side and the sliding material is completely submerged into the water; (e) and (f) show the situation from the front direction.

The wave sensor installed in the model records the wave height. Table 6-1 and Table 6-2 below show the maximum wave recorded for different block arrangements and release height. The wave height is dependent on different parameters. In this study, the wave height is greatly affected by the release height, and the weight, volume, and porosity of the blocks. With the increase of the release height, the volume and the weight of the blocks, the wave height also increased. However, with the increase of porosity for the same

weight of blocks, the wave height decreased; the maximum wave height of Table 6-1 is lower than the maximum wave height of Table 6-2 due to the porosity of the blocks. Generally, the wave height is clearly affected by the block's weight and release height of the blocks. Furthermore, the wave height is affected by the porosity of the block. The still water depth does not have much effect on the maximum wave height. As indicated in Table 6-1 and Table 6-2, the ratio of the maximum wave of the freeboard of 23.7 mm to 31.6 mm of the dam is very close to 1 for both block types. This indicates that the still water depth doesn't have much effect on the maximum wave height. The wave heights recorded by the nine sensors are summarized under Appendix D.

Table 6-1 Maximum wave height to porous block with different block arrangements and release heights for the freeboard of 23.7 mm and 31.6 mm of the dam

Block arrangement	Release height (mm)	Max wave height [mm]		Ratio of $a_{23.7\ mm}/a_{31.6\ mm}$
		Freeboard 23.7 mm	Freeboard 31.6 mm	
1B	1500	61.83	50.05	1.24
	1000	40.82	39.56	1.03
	500	38.74	40.72	0.95
	0	25.01	24.05	1.04
4B	500	83.55	83.08	1.01
	0	63.67	63.96	1
2V	500	49.35	47.87	1.03
	0	31.44	34.15	0.92
2H	0	31.45	33.73	0.93

Table 6-2 Maximum wave height to solid block with different block arrangements and release heights, for the freeboard of 23.7 mm and 31.6 mm of the dam

Block arrangement	Release height (mm)	Max wave height [mm]		Ratio of $a_{23.7\ mm}/a_{31.6\ mm}$
		Freeboard 23.7mm	Freeboard 31.6mm	
1B	1500	58.62	53.42	1.1
	1000	45.42	47.72	0.95
	500	34.25	36.15	0.95
	0	29.85	30.56	0.98
4B	500	104.8	82.06	1.28
	0	93.87	98.57	0.95
2V	500	73.18	64.26	1.14
	0	53.14	53.82	0.99
2H	0	44.17	47.77	0.92

The maximum wave height is recorded on the opposite side of the sliding plane, where the sliding block touches the water's surface in all the performed tests. This means the wave recorded by sensor *1 (CH1) (*Figure 3-1 above) is the maximum for most of the test results. As the generated wave propagates in every direction of the reservoir, it dissipates its energy and the amplitude of the wave also decreased. The pattern of generated wave and

damping of the wave's amplitude for the test no *348* is shown in *Figure 6-2*. As seen from the graph, wave amplitude recorded by sensor *1* is higher than the others and the wave crest is sharp in relation to the other waves' crest. Sensor *7 (CH7)* is located close to the dam's crest. The wave amplitude of sensor *7* is the smallest among the rest of the waves; this is due to the dissipation of energy when a wave propagates. The third wave sensor *(CH4)* is located along the reservoir, in the middle of sensors *1*and *7*. The wave amplitude is greater than sensor *7* but less than sensor *1*.

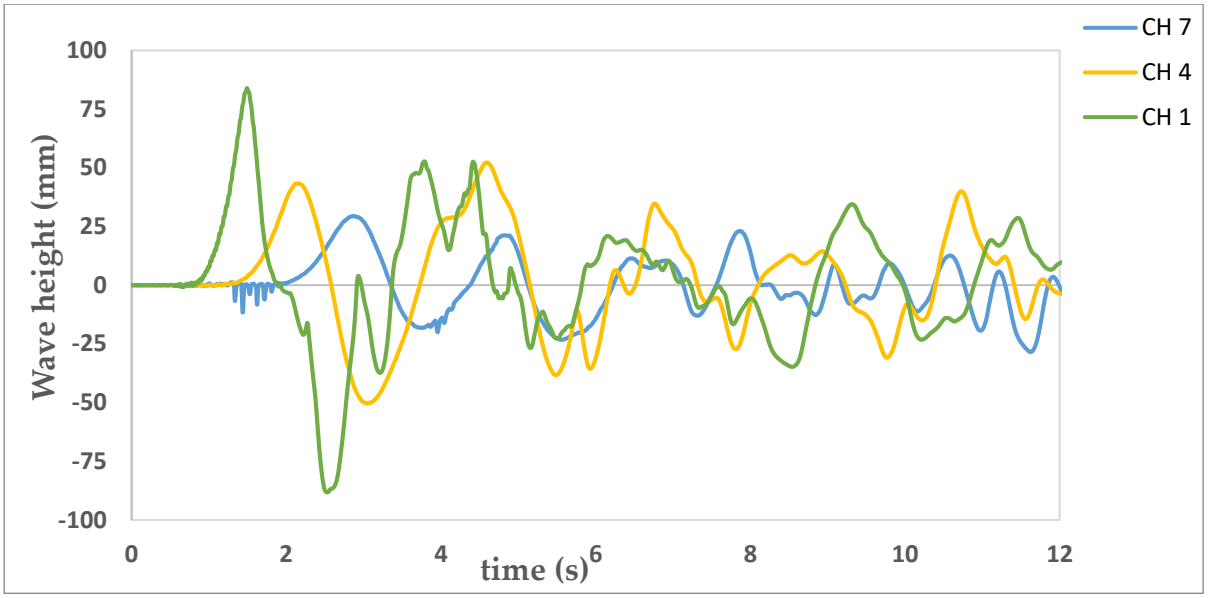

Figure 6-2 The wave amplitude created for three different sensors at different location. It is for test no 348.

Most often the wave created in this study has noise on the wave crest and wave trough. The noise is due to the reflection of the wave that collides with the bank of the reservoir. Due to this reflection the propagated wave isn't smooth. As indicated in Figure 6-2 above, only the first crest and trough are smooth for all of the channels. The maximum height created for the first wave, both for the crest and trough look alike, which is similar to a stock wave's property. The wave generated in this study could be similar to the stock wave type.

6.2 Overtopping Water Volume and Discharge Analysis

The dam structure represents the lowest elevation point in this physical model, simulating a real reservoir. Because of this, it is susceptible to dam overtopping due to a landslide generated wave. The amount of overtopped water volume is one of the main concerns for the analysis of dam safety. Knowing the amount of overtopped water volume is the main parameter in the solution to overcome its effect. In this study, the amount of overtopped water volume is measured manually. There are five buckets that collect the overtopped water from the five different sections of the dam crest. To measure the water volume in the buckets, the bucket is calibrated first; the detailed calibration and the procedure of how to measure the collected water in the bucket are explained in Appendix B

Here a different test set-up is run to study the amount of overtopped water volume both in solid block set-ups and porous block set-ups. Since the aim of this thesis is more concerned with the effect of porous block material, most of the tests are carried out with porous blocks.

The amount of overtopped water volume depends on different parameters. The most common parameters that determine the overtopping volume are; slide impact velocity; the volume of the slide material; the shape of the slide material; the freeboard of the dam; the slope of the upstream face of the dam; and also, the porosity of the material. For both porous and solid block test results from this study, as well as from previous studies of this model, the overtopping water volume varies with the change of these parameters. In addition to the total volume of the water, the distribution of the overtopping water along the dam length is not even. Most often the highest overtopped water volume occurred on both edges of the dam crest. This may cause a high risk for the edge of the dam in the case of a large volume of overtopping. Figure 6-3 shows the distribution of overtopping water volume along the dam crest length for test no. 348. The overtopping distribution in some cases may differ, when the volume of the slide material becomes small and release height is close to the still water level. The maximum overtopping occurs in crest 5.

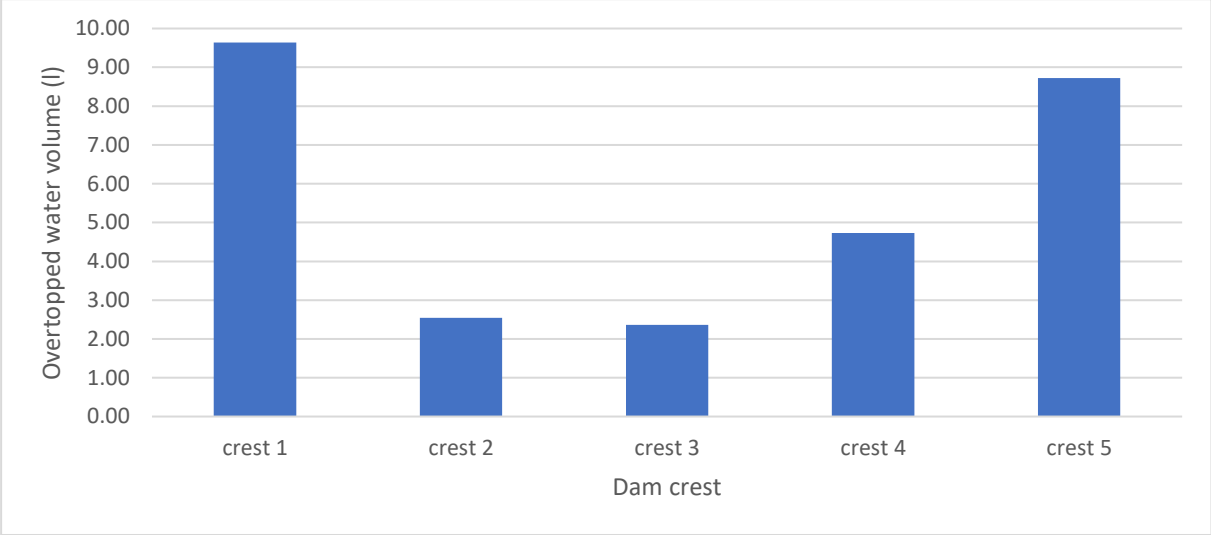

Figure 6-3 The overtopped water volume distribution along the dam crest length. The result is for the porous block test no. 348 with block arrangement of 4B, freeboard (23.68 mm) and 500 mm release height.

As mentioned previously, the overtopped water volume is highly dependent on the block size and the dam freeboards. Both for porous blocks and solid blocks, the effect of the freeboard is shown in Table 6-3 and Table 6-4 respectively. For porous blocks, due to the increase of the freeboard from 23.7 mm to 31.6 mm, the overtopped water volume decreased by 35% to 76% for different release heights. Additionally, for the increase of the block size, the overtopped water volume also increased. Similarly, for solid blocks, due to the increase of the freeboard from 23.7 mm to 31.6 mm, the overtopping water volume decreased by 29% to 80%; which is a slightly higher change as compared to the porous block types. Figure 6-4 clearly shows the effect of the freeboard on the overtopping volume for both porous and solid blocks. Generally, the overtopping volume is dependent on the freeboard of the dam; thus, the freeboard of the dam has a great effect in controlling this overtopping volume.

Table 6-3 The effect of the freeboard on total overtopped water volume for porous blocks with different block arrangements and release height of the blocks

Release height (m)	Block setup	Overtopped volume (l)		Change in volume (%)
		Freeboard of 31.6mm	Freeboard of 23.7mm	
1.5	1B	5.52	8.85	38
1	1B	3.33	5.82	43
0.5	1B	1.21	3.21	62
	2H	3.7	10.12	63
	2V	9.09	14.18	36
	4B	15.88	25.64	38
0	1B	0.18	0.55	67
	2H	0.36	1.52	76
	2V	2.91	4.48	35
	4B	7.94	16.3	51

- 23.7 mm represents for prototype of 4.5 m with a scale of 1:190
  31.6 mm represents for prototype of 6 m with a scale of 1:190

Table 6-4 The effect of the freeboard on total overtopped water volume for solid blocks with different block arrangements, and release height of the blocks

Release height (m)	Block setup	Total overtopped volume (l)		Change in volume (%)
		Freeboard of 31.6mm	Freeboard of 23.7mm	
1.5	*1B*	10.36	15.27	32
1		5.94	8.42	29
0.5		3.21	5.33	40
0	*1B*	0.18	0.91	80
	2H	0.42	2.18	81
	2V	7.21	12.79	44
	4B	14.36	35.76	60

- *23.7 mm represents for prototype of 4.5 m with a scale of 1:190*
  31.6 mm represents for prototype of 6 m with a scale of 1:190

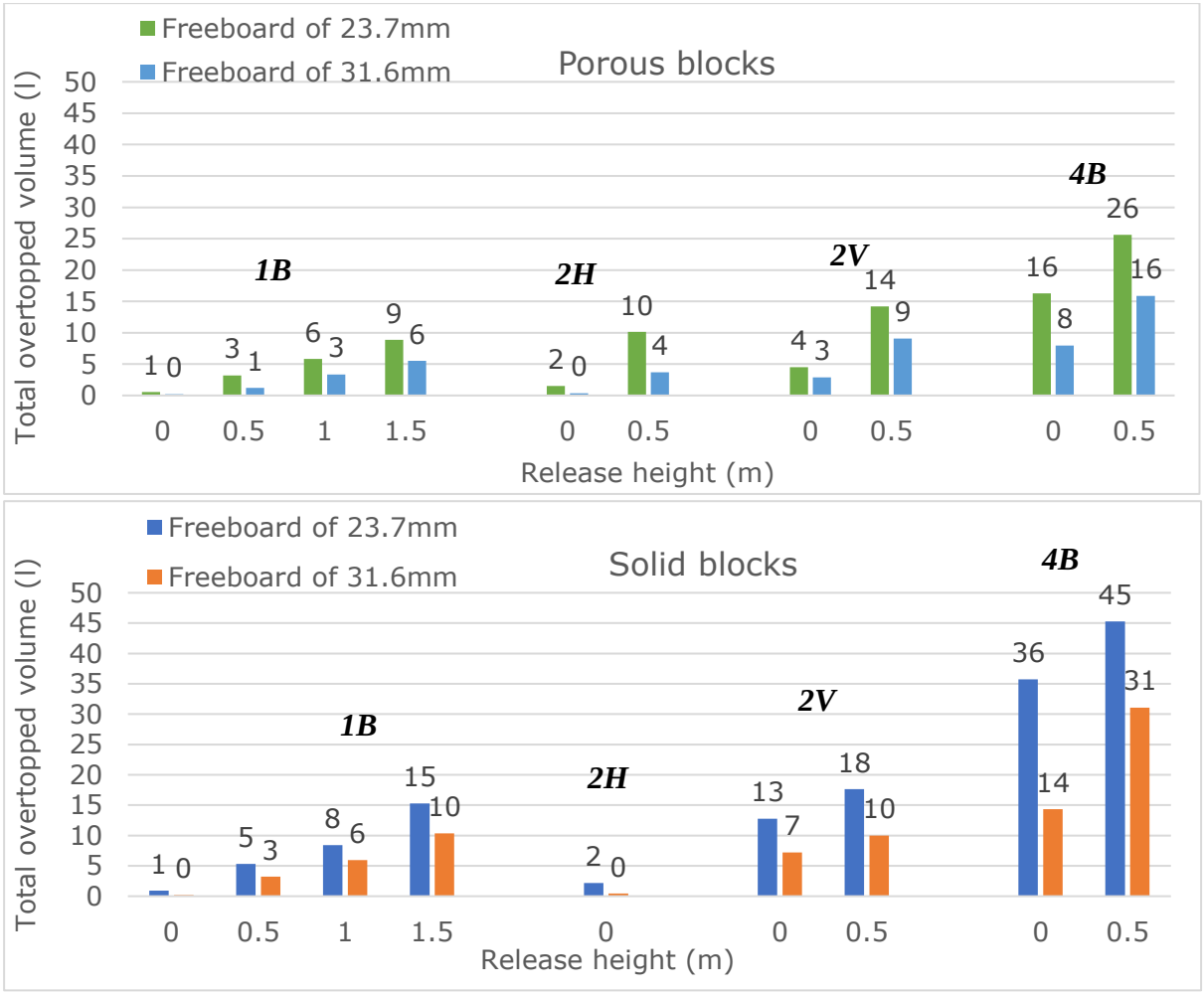

Figure 6-4 Total overtopped volume comparison for the freeboard 23.7 mm and 31.6 mm, (for both porous and solid blocks); 23.7 mm represents prototype of 4.5 m while 31.6 mm represents for prototype of 6 m.

Discharge is another parameter that is useful for investigating the effect of the overtopped water volume. The effect of overtopped water depends on the rate of flow over the dam crest and for how long the discharge rate remains flowing. The overtopping discharge remained flowing for 15 to 25 seconds in most of the test outputs. In this study, average discharge analysis is performed for each subdivided dam crest separately; which may not give the exact value of the discharge rate, but it can show the average discharge value. The average discharge can be analyzed, since the amount of overtopped water volume is known and the time it takes is also recorded. From this known data the average discharge will be calculated by dividing the volume by the time elapsed. In this analysis, there is some uncertainty. One of the main uncertainties is that the overtopped water is not continuous; it flows over the dam in the form of a wave. So, there is a gap between two consecutive overtopped water waves. Also, the overtopping distribution along the dam length is not even because this overtopping discharge rate is not similar over the dam length. The discharge analysis for test no. *348* is shown in Table 6-5; for this test result the overtopping distribution along the dam crest is indicated in Figure 6-3 above.

Figure 6-5 shows the time gap between two consecutive overtopping waves when overtopping is not occurring. For example, crest 4 overtopping starts at 3.3 s, stops at 4 s and restarts again at 6 s. This shows that there is no overtopping between 4 and 6 s. Table 6-5 shows the average discharge along the dam crest. As seen from the result, the average

discharge is not similar along the dam length. The highest average discharge occurs on the edge of the dam crest. Most often the largest average discharge occurs at the edge of the dam crest. For this test result the maximum average discharge occur at crest 5.

Table 6-5. This table shows the variation of average discharge along the dam crest. It is for test no. *348,* block arrangement of *4B*, freeboard of *23.7 mm*, and *500 mm* release height.

Dam crest	*V_{total} (l)*	*t_1 (sec)*	*t_2 (sec)*	*dt*	*Q_{avg} (l/s)*
Crest 1	9.64	3.2	13.8	10.6	0.91
Crest 2	2.55	3.2	10	6.8	0.37
Crest 3	2.36	3.2	11.5	8.3	0.28
Crest 4	4.73	3.3	9.8	6.5	0.73
Crest 5	8.73	3.3	9.7	6.4	1.36

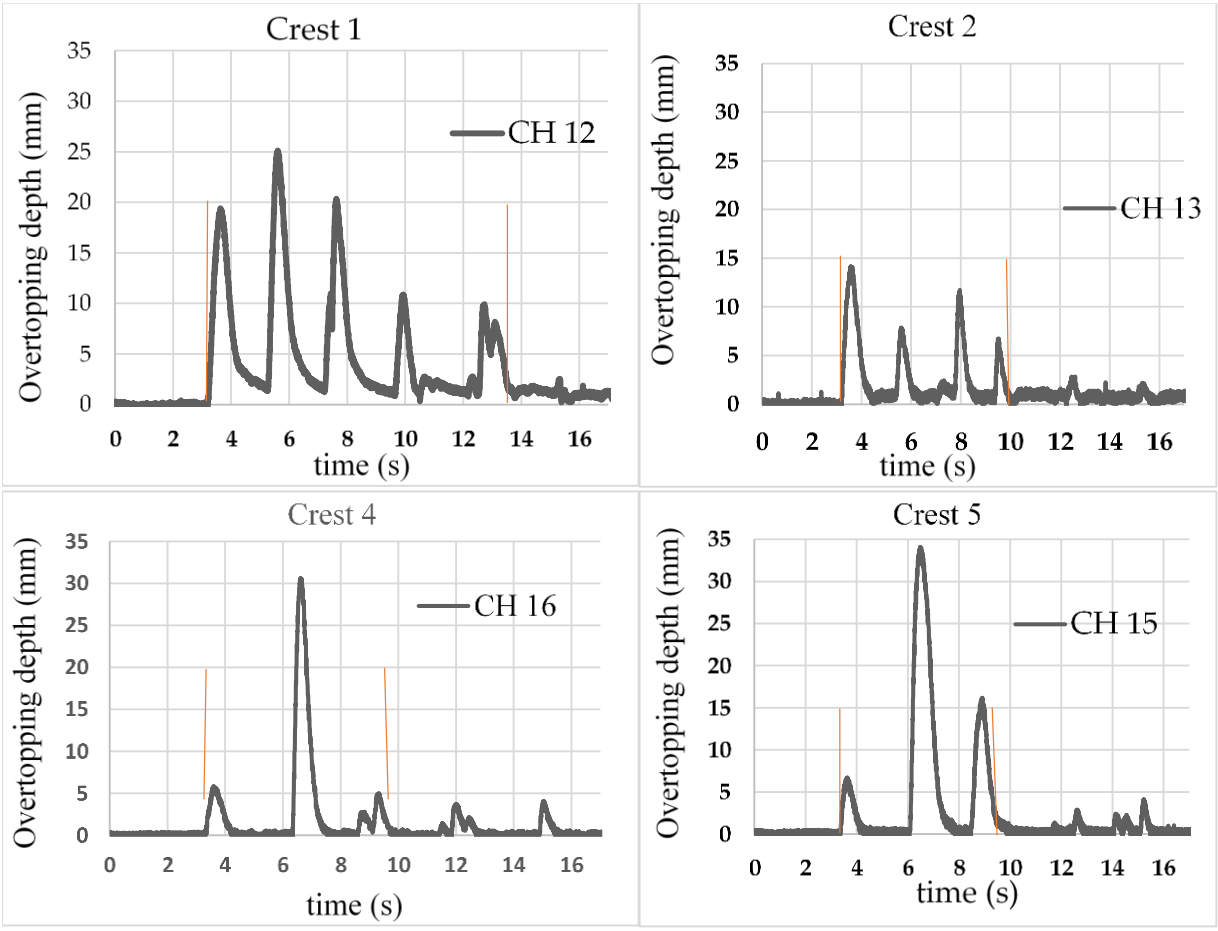

Figure 6-5 This figure shows the pattern of the overtopping discharge along the dam crest and the discontinuity of overtopping wave.

6.3 Analysis of Maximum Overtopping Depth Over the Dam Crest

Maximum overtopping depth is one of the key variables in the analysis of dam overtopping (Kobel et al., 2017). In this study, the overtopping depth over the dam crest is recorded by five ultrasonic sensors. The impact of the weight of the block, the release height of the block, and the depth of the still water on the maximum overtopping depth is analyzed. The maximum overtopping depth is greatly affected by the release height of the block. For both freeboards of the dam shown in Figure 6-6, with the increase of the release height from 0 to 0.5 m the maximum depth created increased, approximately by half for all block arrangements, except the 4B block arrangement. Although with the increase of the weight of the sliding block, the maximum overtopping depth increased. The depth of the still water has a moderate influence on the maximum overtopping depth created over the dam crest. As shown in Figure 6-6, with the increase of the freeboard of the dam the overtopping depth decreased to some extent. For this model, increasing the freeboard is the same as decreasing the depth of the water.

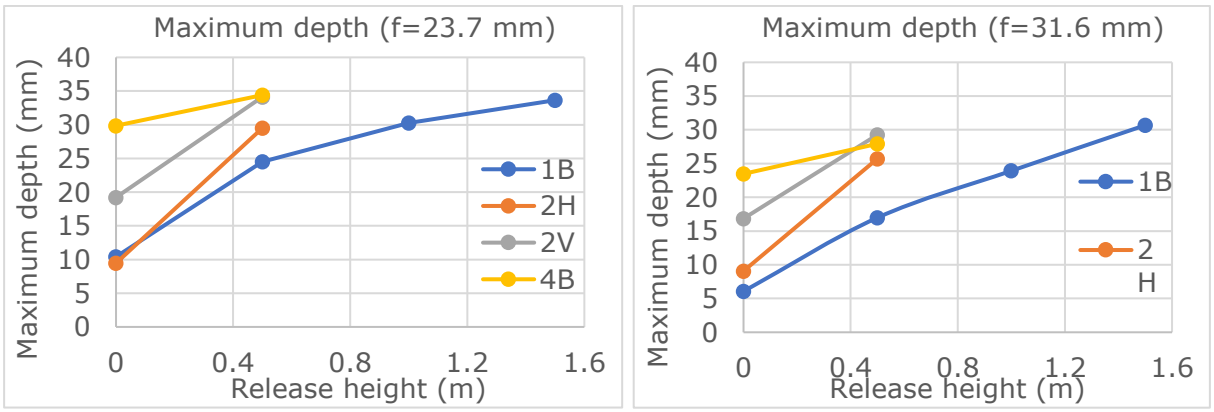

Figure 6-6 This figure shows the impact of release height, weight of the block, and freeboard of the dam on the maximum overtopping depth created over the dam crest; the result is for porous blocks

6.4 Slide Impact Velocity Analysis and Impact of Velocity on Overtopping Volume and Overtopping Depth

Impact velocity is the velocity of sliding material when it touches the water's surface (Heller et al., 2009). The landslide impact velocity is influenced by the starting position of the slide on the ramp. When the starting position of the sliding material is far from the still water level (elevation difference between still water level and center of gravity of sliding material increased) the kinetic energy due to the material will be increased. When the sliding material hits the water's surface, it transfers the momentum (kinetic energy) into wave energy (McFall and Fritz, 2016). The velocity in kinetic energy has a great influence since velocity is squared ($Ek = \frac{1}{2}mv^2$). Therefore, the slide impact velocity is exceedingly dependent on the starting position of the slide material on the ramp.

The slide impact velocity might be evaluated in different ways; according to Heller et al (2009) the impact velocity is calculated with a formula:

$$Vs = \sqrt{2g\Delta Zsc(1 - tan\,\delta\, cot\,\alpha)} \quad \text{6-1}$$

where

- $g\ (^{m}/_{s^2}) -$ gravitational acceleration; $g = 9.81\ ^{m}/_{s^2}$
- $\Delta Zsc\ (m)$ –height of the center of gravity of the slide. It is the vertical distance between the center of gravity of a mass in the original position and the impact location (the water surface).
- $\alpha -$ slide impact angle. It is the inclination angle of the sliding plane from the horizontal surface. For this model it is 50°.
- $\delta -$ dynamic bed friction angle. It represents the friction at the contact between the slide mass and the sliding plane; which normally falls in the range of $15^o\ to\ 35^o$ (Heller et al., 2009).

From the output data of the laboratory result, the velocity of the slide block is calculated from the *S-t* series data. The position of the sliding block from the initial point to the end (when the block stops) with respect to time is recorded. Taking the starting point as zero for both the time and position of the block, the velocity of the sliding block is calculated using the velocity formula ($Vs = \frac{dS}{dt}$). To calculate the velocity using equation 6.1 mentioned above the center of gravity of the sliding block must be known. For test number 348, the position of the sliding blocks from the initial to the final position and the corresponding velocity of the blocks is shown in Figure 6-7. The maximum velocity of the block is recorded either when the sliding material touches the water's surface or after the time taken for the initial touch. After the sliding material touches the water's surface, the buoyancy force is applied to the object, which resists the object's gravitational force; thereby, the rate of the object's speed increment starts to decrease. At some point the increment rate will change to a decreasing rate. The point at which the increment rate changes is recorded as the maximum velocity of the object. In most cases, the maximum speed of the block for this study was recorded close to when the block touched the water's surface.

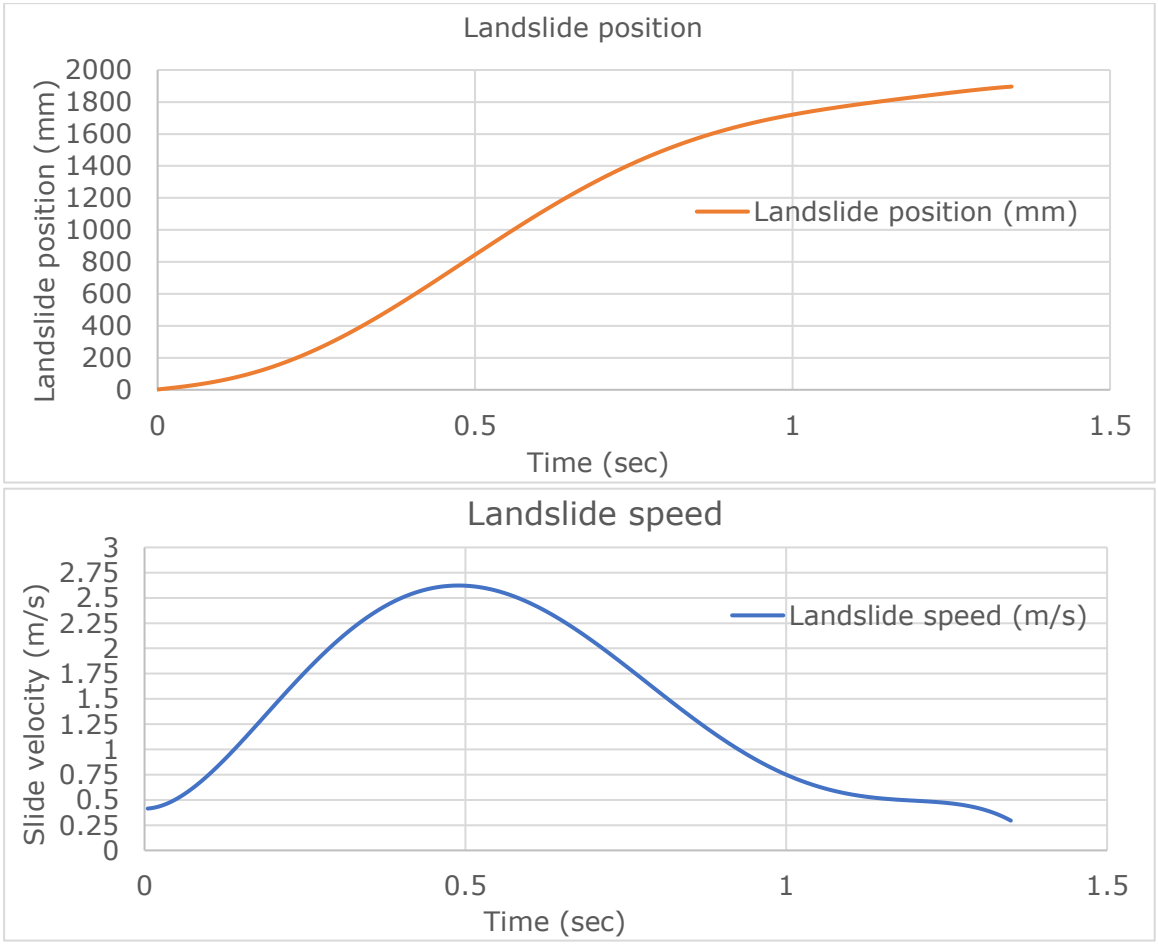

Figure 6-7 This diagram shows the position of the sliding block and the corresponding speed. It is taken from test no. 348 with block configuration 4B, and release height of 500 mm.

Impact velocity is one of the main factors that control the overtopping water volume and maximum water depth created on the dam crest during overtopping. The overtopped water volume increased as the impact velocity increased in all the tests' output. The distribution of overtopped water volume is clearly affected by the weight and volume of the sliding blocks. As indicated in Figure 6-8, for block configuration of *4B*, the maximum overtopped water is through crest *1*; while in the rest of the block configurations the maximum overtopping occurs through crest *5*. In both cases maximum overtopping occurs on the edge of the dam crest. This is similar in the case of solid blocks as well. It is indicated in Appendix C.

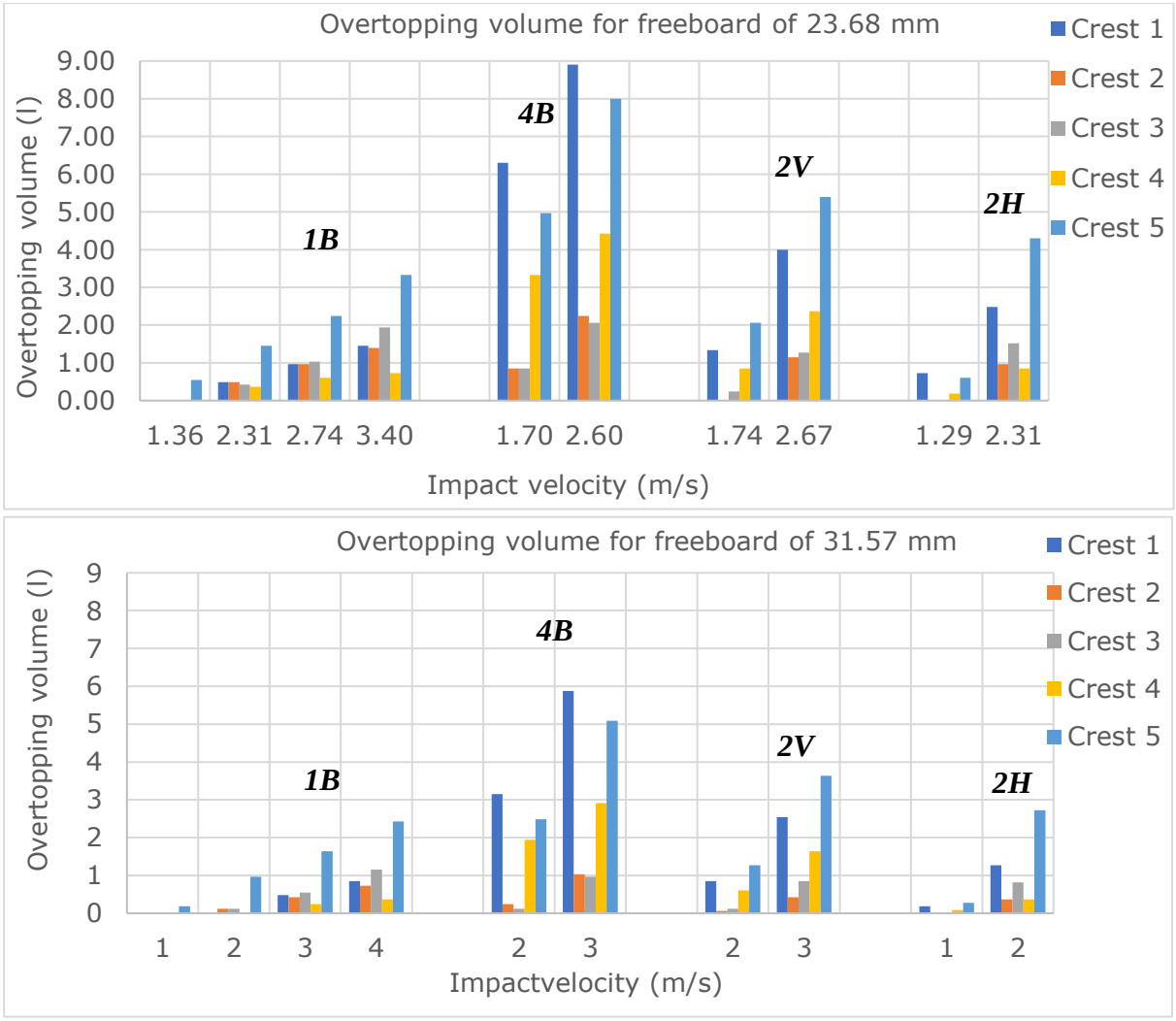

Figure 6-8 This figure shows the effect of impact velocity on the overtopping volume distribution along the dam crest. It is for porous block types.

The maximum overtopping depth is directly proportional to the impact velocity. It is clearly shown in Figure 6-9 that as the impact velocity increases the maximum overtopping depth also increases. The weight and volume of the sliding blocks have an effect on the maximum overtopping depth along the dam crest. As shown in Figure 6-9(a) and (c), the depth created on crest 4 for the block configuration of 1B is the smallest compared to the other part of the dam crest. However, for block configuration of 4B, it is the second-highest value. The situation is similar for both the freeboards of the dam. It can be concluded that the place where the maximum overtopping depth is created, is affected by the volume and weight of the sliding blocks for the fixed reservoir geometry.

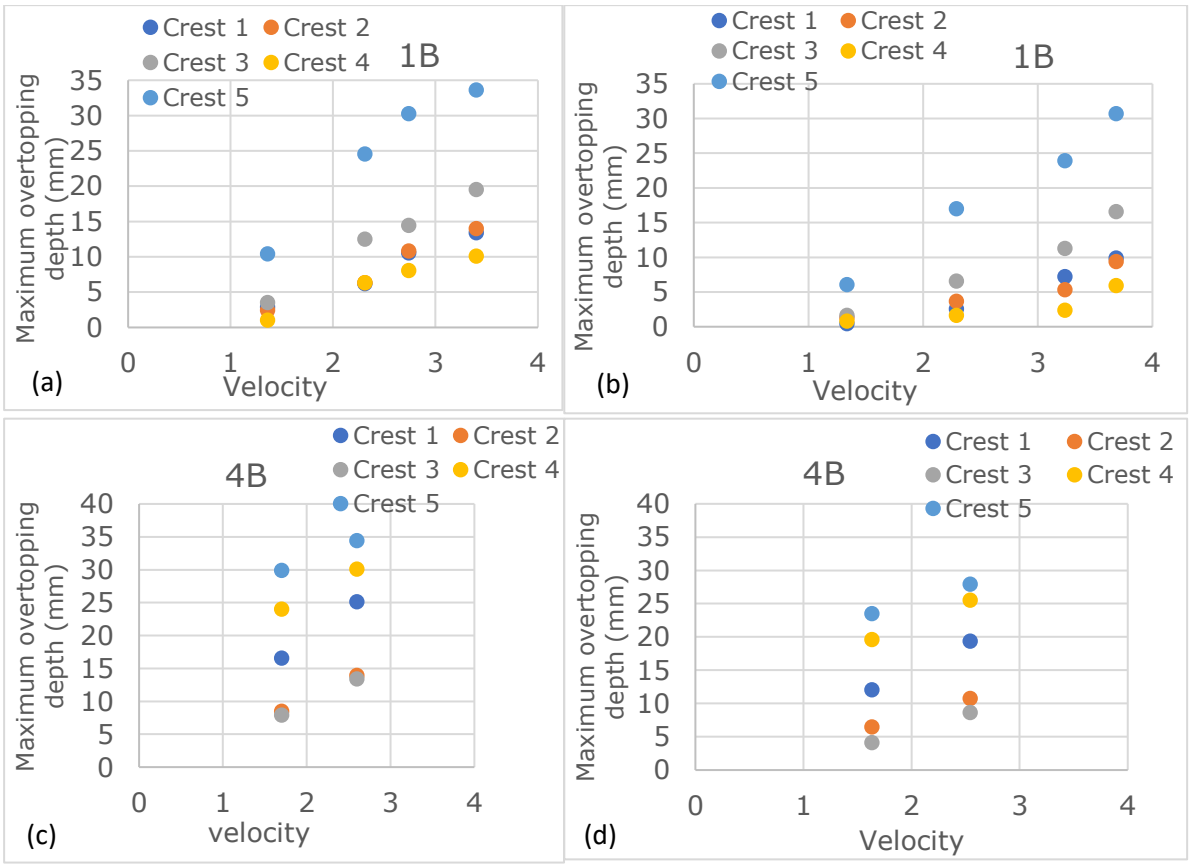

Figure 6-9 Effect of impact velocity on the maximum overtopping depth for porous blocks, block configuration of 1B and 4B; (a) and (c) are for the freeboard of 23.68 mm; while (b) and (d) are for the freeboard of 31.57 mm

6.5 Comparison of Porous and Solid Blocks

6.5.1 Comparison of Generated Wave

The situation of the generated wave for both porous and solid blocks is described in section 6.1. In this section, the effect of the porosity of the block on the wave created is analyzed. Table 6-6 summarizes the ratio of the maximum wave created for solid blocks and porous blocks. As shown in the table, the ratio ranges from 0.88 to 1.67. This indicates that the maximum wave created by the solid block is larger than by the porous block, except for some block combinations which are below 1 but close to 1. In most of the results the ratio is above 1. It can be concluded that the porous block generates less, or an equal wave compared to solid blocks.

Figure 6-10 presents a comparison of waves created at different locations of the reservoir. The blocks have a similar configuration and release height. The main difference between the blocks is the porosity of the material. As observed from Figure 6-10, the general wave features at different locations of the reservoir have a similar pattern; but the maximum wave amplitude recorded for the porous block is smaller compared to the solid blocks. It can be concluded from this observation that changing the porosity of the material has a negligible effect on the wave features. However, the porosity of the material has a clear effect on the wave amplitude.

Table 6-6 Comparison of maximum wave created for both solid and porous blocks

Freeboard *(mm)*	Block arrangement	Release height (mm)	Max wave height *[mm]*		$\frac{aM\ block}{aM\ porous}$
			Porous blocks	Solid blocks	
23.7	*1B*	1500	61.83	58.62	0.95
		1000	40.82	45.42	1.11
		500	38.74	34.25	0.88
		0	25.01	29.85	1.19
	4B	500	83.55	104.80	1.25
		0	63.67	93.87	1.47
	2V	500	49.35	73.18	1.48
		0	31.44	53.14	1.69
	2H	0	31.45	44.17	1.40
31.6	*1B*	1500	50.05	53.42	1.07
		1000	39.56	47.72	1.21
		500	40.72	36.15	0.89
		0	24.05	30.56	1.27
	4B	500	83.08	82.06	0.99
		0	63.96	98.57	1.54
	2V	500	47.87	64.26	1.34
		0	34.15	53.82	1.58
	2H	0	33.73	47.77	1.42
13	*1B*	500	35.61	44.87	1.26
	2H	500	55.87	72.15	1.29
	2V	500	58.58	77.05	1.32
	4B	500	93.60	127.79	1.37

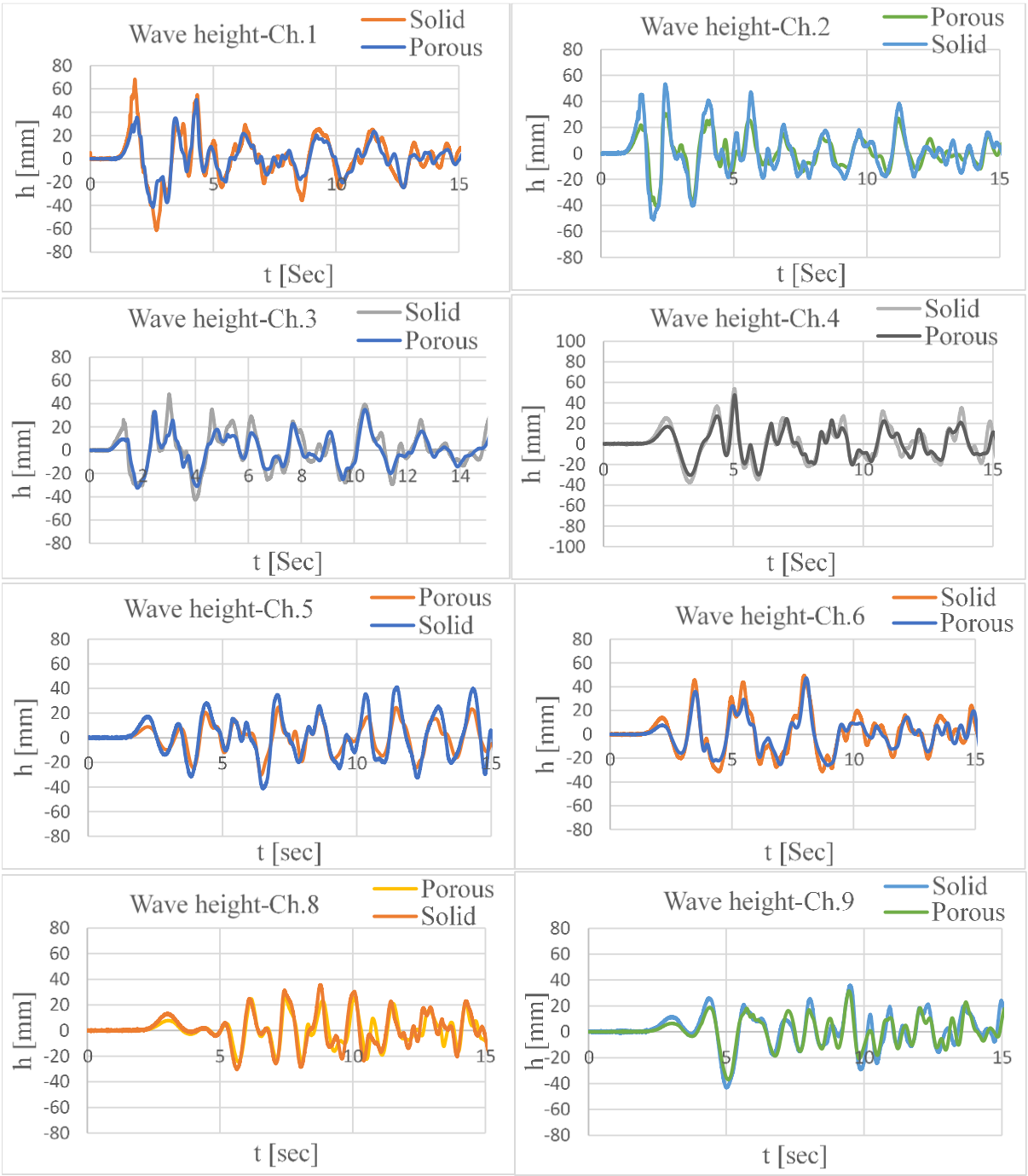

Figure 6-10 This figure shows the wave pattern of both porous and solid blocks. It is from tests no. 287 (solid block) and 335 (porous block). It has a block configuration of 1B and a release height of 1.5 m.

6.5.2 Overtopping Volume Comparison

As mentioned in section 6.2, the overtopping distribution along the dam crest was not similar for both porous and solid blocks. Figure 6-11 and Figure 6-12 below show the comparison of total overtopping volume for porous and solid blocks. The comparison is made for blocks with similar weights and block arrangements, for two different freeboards of the dam. As observed from the result, for all block combinations the total overtopped water volume for the solid block is larger than for the porous blocks. This shows that the porosity of the sliding block clearly affects the total overtopping water volume during

landslides to reservoirs. From the result of this study, blocks with high porosity generate less overtopping in all block combinations; even if the material has a similar weight. However, the rate of volume change is not similar for all block arrangements. As observed from the result, the effect of porosity on block 4B is much higher than the rest of the block combinations. It is clearly observed that the incremental volume change for block combination 4B looks higher. Generally, it can be concluded from the bar chart that porous blocks generate less overtopping volume than solid blocks. Additionally, the effect of porosity on overtopping volume increases with the increase of the block weight and the volume of the materials.

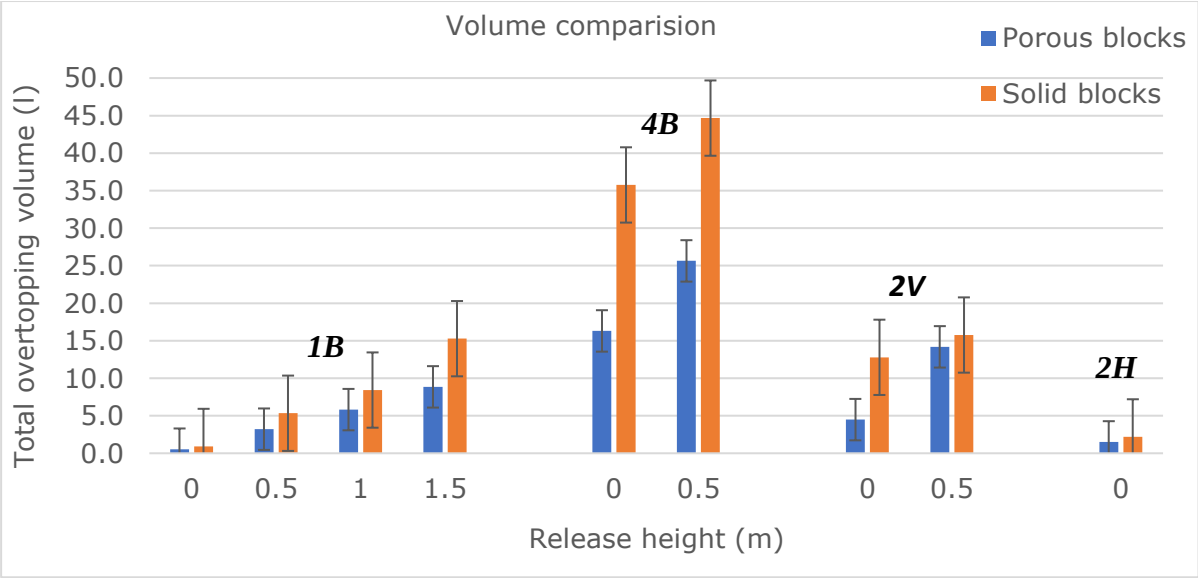

Figure 6-11 Comparison of overtopped volume for solid and porous blocks with similar weight (freeboard =23.68 mm)

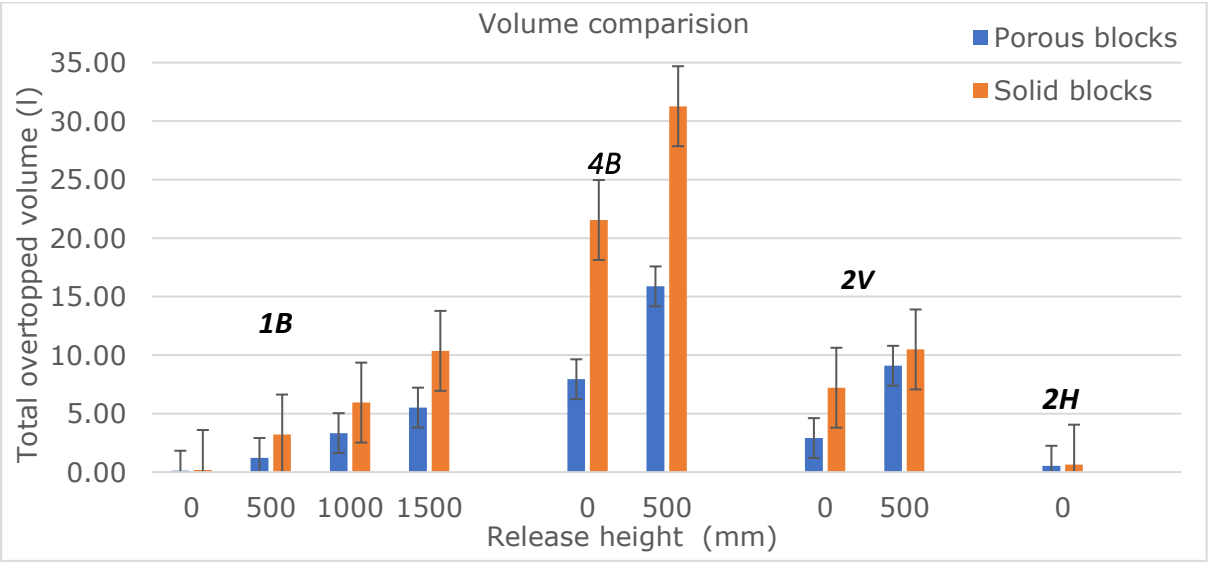

Figure 6-12 Comparison of overtopped volume for solid and porous blocks with similar weight (freeboard =31.6 mm)

6.5.3 Maximum Overtopping Depth Comparison

The maximum overtopping depths of the five segments of the dam crest are not similar. Most often the maximum overtopping depth is recorded where the highest overtopping volume is created. Sometimes this is not the case, and the maximum depth is recorded irrespective of the overtopping volume. The maximum depth created is greatly dependent on the starting point (release height) of the blocks for both block types. For the porous blocks the maximum overtopping depth increases with the increase of the release height. This is shown in Figure 6-13 and Figure 6-14 for all block configurations. The trend of the maximum height created for the solid block is not similar to the porous blocks. For the same block arrangements with the increase of the release height, the maximum overtopping depth is decreased. For the block arrangements of 4B, 2V, and 1B, with the increase of the release height there was a situation where the maximum depth created decreased. The porosity of the slide material influences the maximum overtopping depth created. However, it is difficult to conclude whether the porosity of the material either decreases or increases the maximum depth created along the dam crest. Since the result of this study shows that the maximum depth created due to porosity change only, does not have a similar trend in different block combinations. As per the result in Figure 6-13 and Figure 6-14 for block combinations of 1B with a release height of 0.5 and 1 m, the maximum depth created for the solid block is higher than the porous blocks; but for block combination of 1B with a release height of 0 m and 1.5 m, the maximum depth created for the solid blocks is lower than for the porous blocks. This situation is similar for block combinations of 4B and 2V. From this study's result, it can be concluded that the maximum depth created along the dam crest with the porous block would be less or greater than the maximum depth created with solid blocks. To have a better understanding of this situation, it is best to perform additional tests with different parameter combinations

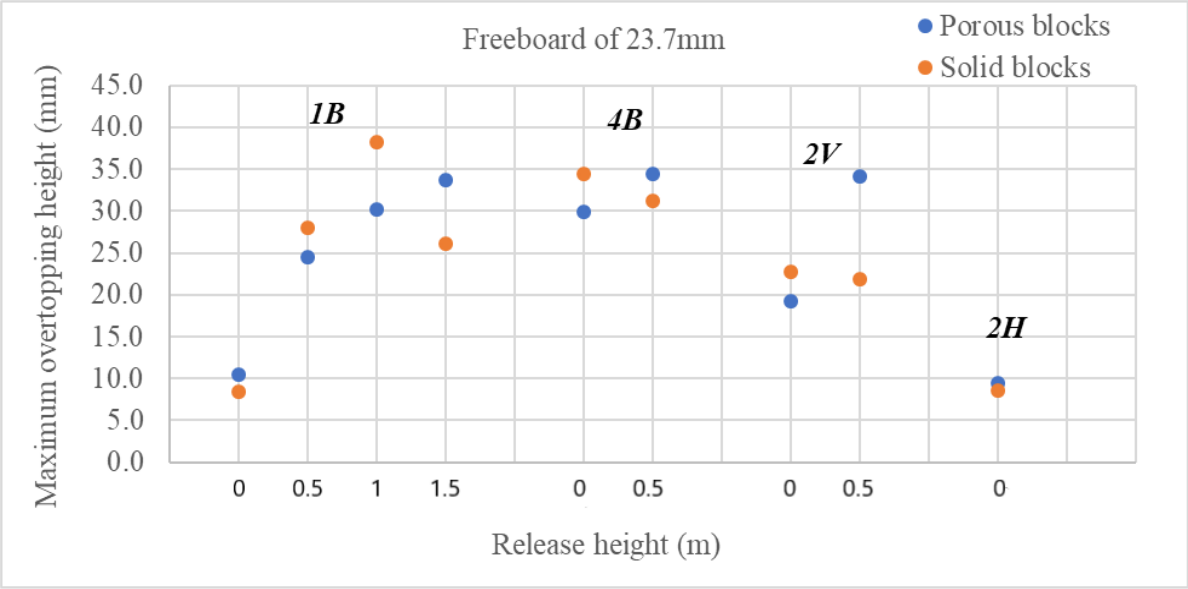

Figure 6-13 Comparison of maximum overtopping depth created for porous and solid blocks with a freeboard of 23.7 mm and different block combinations

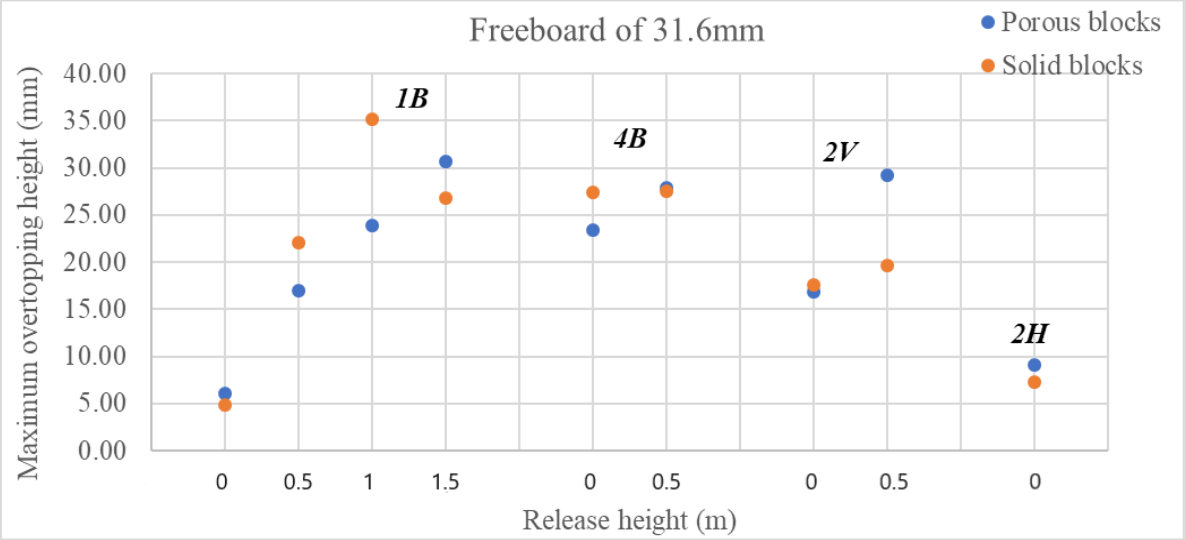

Figure 6-14 Comparison of maximum overtopping depth created for porous and solid blocks with a freeboard of 31.6 mm and different block combinations

6.6 Comparison with Kobel et al., (2017)

6.6.1 Comparison of Maximum Overtopping Depth

A comparison of the maximum overtopping depth is made to the equation of Kobel et al., (2017). The equation is applied for a two-dimensional (2D) solitary wave type and impulse wave overtopping on a rigid structure. According to their equation, the maximum overtopping depth is dependent on different parameters. They conclude that the wave amplitude has a dominant effect, whereas the relative still-water depth has a medium effect. The equation proposed by Kobel et al., (2017) is given as below. The main difference is that one equation includes the upstream dam face slope effect and the other excludes the effect (Kobel et al., 2017)

$$\frac{do}{w} = 1.34\left[\varepsilon\left(\frac{h}{w}\right)^{1.7}\left(\frac{\beta}{90^0}\right)^{0.25}\right] = 1.34E1; \quad 0.4 < E1 < 0.7 \ldots\ldots\ldots\ldots\ldots\ldots\ldots\ldots\ldots\ldots\ldots\ldots\ldots\ldots\ldots\ldots\ldots\ldots\ldots\ldots\ldots\ldots 6\text{-}2$$

$$\frac{do}{w} = 1.32\left[\varepsilon\left(\frac{h}{w}\right)^{4\left[\left(\frac{\beta}{90^0}\right)^{-0.21-\varepsilon}\right]}\left(\frac{\beta}{90^0}\right)^{0.16}\right] = 1.32E2; \quad 0.1 < E2 < 0.7 \ldots\ldots\ldots\ldots\ldots\ldots\ldots\ldots\ldots\ldots\ldots\ldots\ldots\ldots\ldots\ldots\ldots\ldots\ldots\ldots 6\text{-}3$$

where

do……. Maximum over topping depth

w…… Dam height

ε……. Relative wave amplitude (a/h)

h……..…… Still water depth

β……..…… Upstream dam face angle

As per Kobel et al., (2017) for the still water depth ranging between *0.1 to 0.3* m the relative wave amplitude (*ε*) should be in the range of *0.1 to 0.7* in order to generate waves. For this study, the still water depth is within the range of *0.25 to 0.295 m*, which is in the range of Kobel et al., (2017) assumption. The calculated value of '*ε'* is in the minimum

range *(*~0.1*)*. Since the value of "*E*" is less than *0.4* for all calculations in this study, equation *6.3* shown above is used for the comparison. To calculate the relative wave amplitude, the amplitude of the wave recorded in front of the dam is used. There are test results that didn't fulfill the criteria. The comparison is made for test results which fulfill (Kobel et al., 2017) criteria. The comparison of the results is illustrated in Figure 6-15 (porous block) and Figure 6-16 (solid block). For porous blocks, some of the calculated maximum depth results are very close to the measured value. For both freeboards of *23.7 mm* and *31.6 mm*, the result of the calculated value is close to the measured value, except for the block combination of *2V* with a release height of *500 mm*. The summary of the comparison is illustrated in Appendix A.

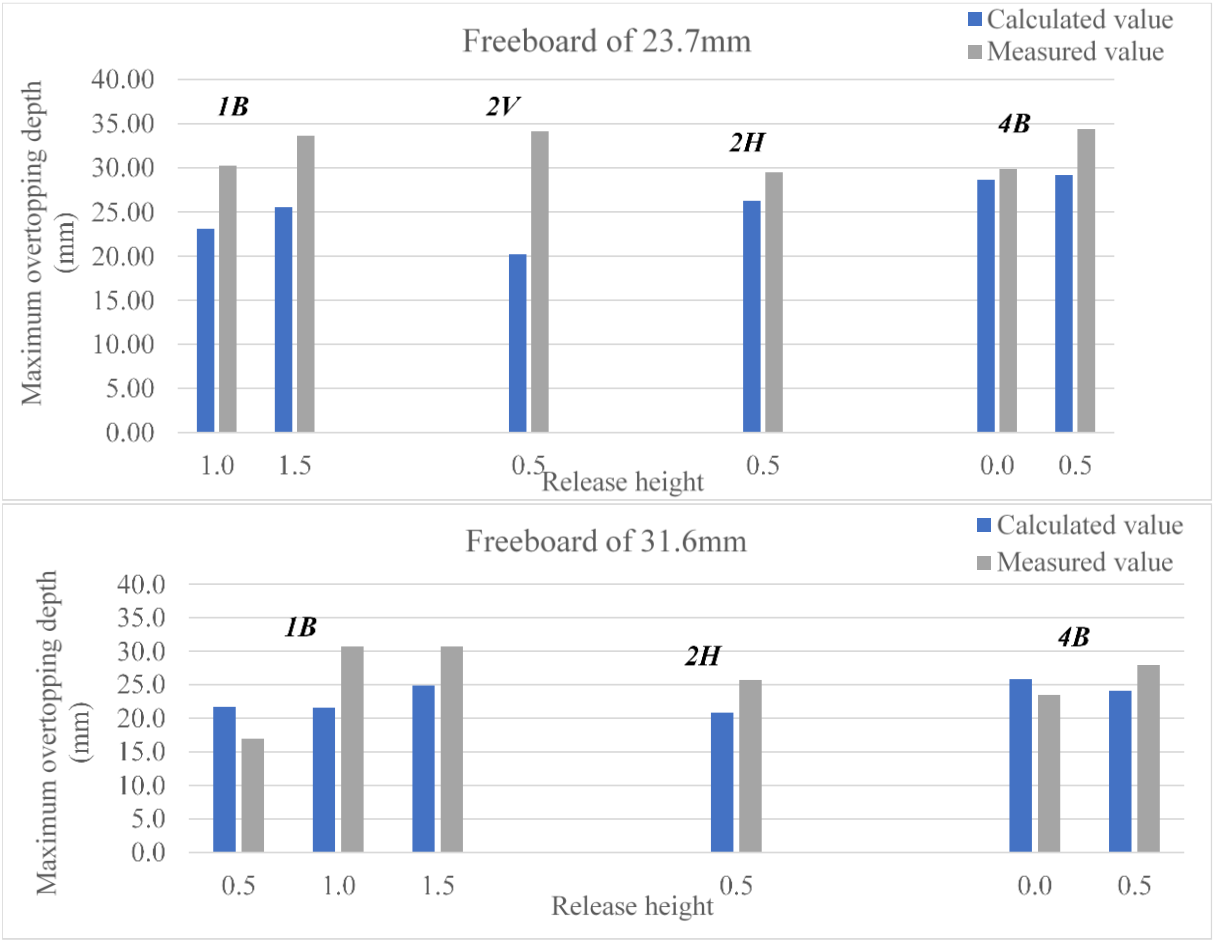

Figure 6-15 This figure shows the comparison of maximum overtopping depth created with porous blocks to the equation developed by Kobel et al., (2017), for a freeboard of 23.7 mm, and 31.6 mm with different release heights

For solid blocks the calculated overtopping value is less, equal and greater than the measured value. It doesn't have a similar trend for different block configurations. For a freeboard of a *68.4 mm* dam Kobel et al., (2017) result overestimated, compared to the actual measurement. The comparison result is shown in Figure 6-16.

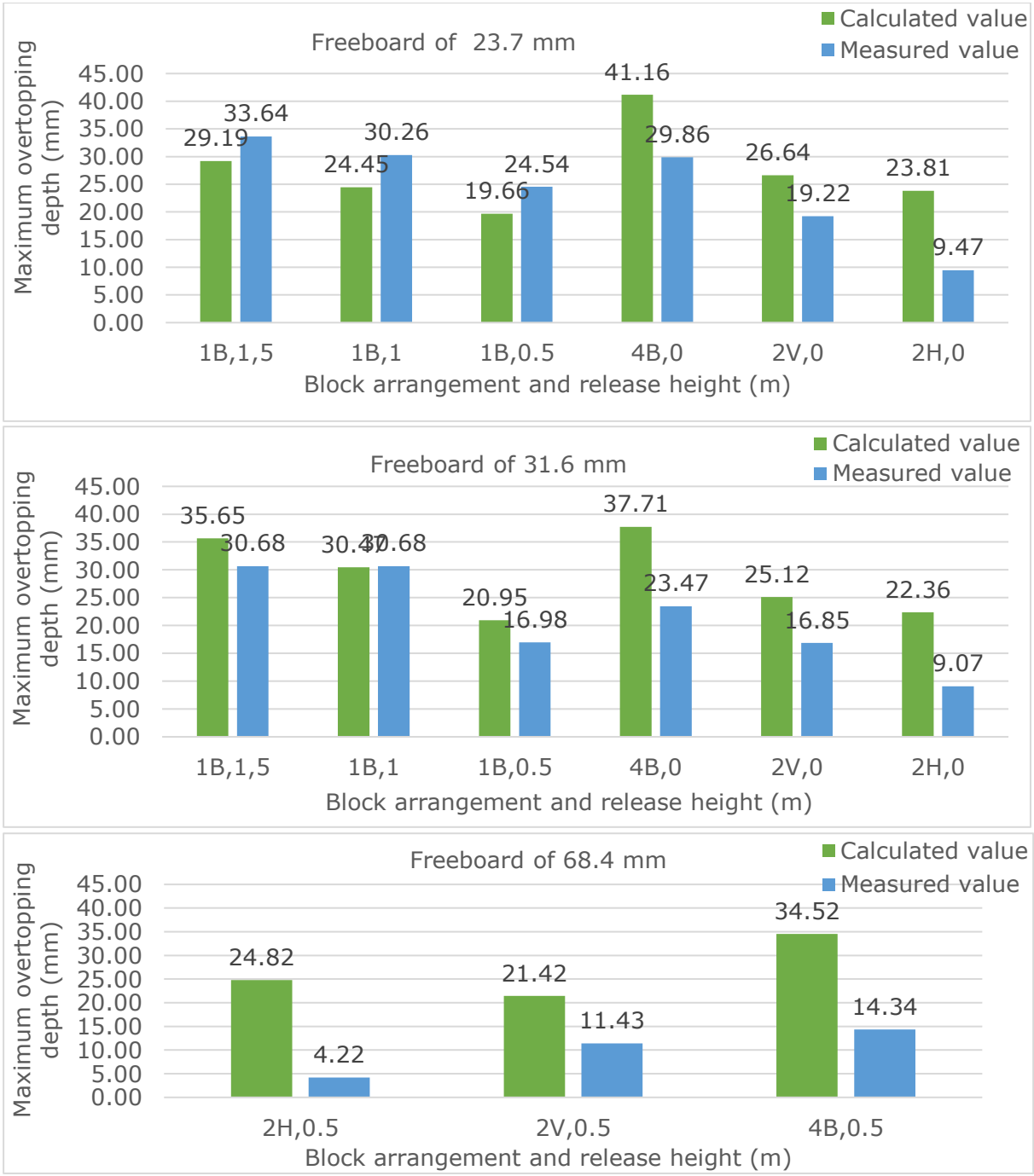

Note 1 The X axis is in the form of (x, y); where x represents block configuration, and y represents release height.

Figure 6-16 This figure shows the comparison of maximum overtopping depth created with solid blocks to the equation developed by Kobel et al., (2017); for freeboards of 23.7 mm, 31.6 mm, and 68.4 mm with different release heights

6.6.2 Comparison of Overtopping Volume

In addition to the maximum overtopping depth calculation formula, (Kobel et al., 2017) developed the overtopping volume calculation formula. They developed two overtopping volume calculation formulae. The main difference between the formula is that one considers the effect of the upstream dame slope and the other neglect this effect The equation which considers the upstream dam face slope effect has R^2 of 0.99; while that which excludes the upstream dam slope effect has R^2 of 0.96 (Kobel et al., 2017).

$$\frac{V}{bh^2} = 1.42\left[\varepsilon * \left(\frac{h}{w}\right)^{2.5}\left(\frac{aw}{bk}\right)^{0.105}\right]^{0.8} = 1.42W1^{0.8} \ldots\ldots\ldots\ldots\ldots\ldots\ldots\ldots\ldots\ldots\ldots\ldots\ldots\ldots\ldots\ldots\ldots\ldots\ldots\ldots\ldots\ldots\ldots\ldots\ldots\ldots 6\text{-}4$$

$$0.35 < w1^{0.8} < 0.95, 0.07 < \frac{bk}{w} < 0.53 \text{ (Kobel et al., 2017)}$$

$$\frac{V}{bh^2} = 1.35\left[\varepsilon * \left(\frac{h}{w}\right)^{\left(\frac{2}{\varepsilon}\right)\left(\frac{\beta}{90}\right)^{0.25}}\left(\frac{aw}{bk}\right)^{0.12}\right]^{0.7} = 1.35W2^{0.7} \ldots\ldots\ldots\ldots\ldots\ldots\ldots\ldots\ldots\ldots\ldots\ldots\ldots\ldots\ldots\ldots\ldots\ldots\ldots\ldots\ldots\ldots\ldots\ldots\ldots 6\text{-}5$$

$$0.15 < W2^{0.7} < 0.95, 0.07 < \frac{bk}{w} < 0.53 \text{ (Kobel et al., 2017)}$$

In this study, the formula that considers the upstream dam slope (equation 6.5) is used. For the calculation of the relative wave amplitude (ε), the maximum wave amplitude in front of the dam is used. Most of the test results didn't fulfill Kobel et al., (2017) criteria; but for those results which did fulfill their criteria, a comparison is done. Table 6-7 and Table 6-8 show the comparison of overtopped water volume with Kobel et al., (2017) equation for porous and solid blocks respectively. As indicated in the tables, the ratio of $V_{Kobel}/V_{measured}$ is in the range of 1.46 to 2.7. This shows that Kobel et al., (2017) equation overestimates the overtopping volume compared to the actual measurement.

Generally Kobel et al., (2017) overestimated the overtopping water volume, but a close estimation for the calculation of the maximum depth above the dam crest was given.

Table 6-7 Porous block, overtopping volume comparison to Kobel et al., (2017) equations

Freeboard (mm)	Block arrangement	Release height (mm)	Overtopped volume (Kobel's) Volume (*l*)	Overtopped volume Measured volume (*l*)	$V_{Kobel}/V_{measured}$
23.68	4B	500	41.46	25.64	1.62
	4B	0	40.2	16.3	2.47

Table 6-8 Porous block, overtopping volume comparison to Kobel et al., (2017) equations

Freeboard (mm)	Block arrangement	Release height (mm)	Overtopped volume (Kobel's) volume (l)	Overtopped volume Measured volume (l)	$V_{Kobel}/V_{measured}$
23.68	1B	1500	41.49	25.64	1.62
	4B	0	69.32	25.64	2.70
	2V	0	35.34	16.3	2.17
31.57	1B	1500	49.68	25.64	1.94
	1B	1000	37.56	25.64	1.46
	4B	0	54.38	25.64	2.12

7 Conclusion and Recommendation

7.1 Conclusion

The main focus of this study was to investigate dam overtopping due to waves generated by landslides into reservoirs and compare the experimental results of porous blocks and solid blocks. The landslide material is simulated by these porous blocks and solid blocks. The influence of different parameters on the overtopping volume, overtopping depth, and the generated wave was studied. Then a comparison of the experimental results from the porous blocks and solid blocks on the generated wave, overtopping volume, and overtopping depth along the dam crest was analyzed. For this study, a total of 123 tests were performed for both the porous and solid blocks. Based on the test results' analysis, the following conclusions are drawn.

- The generated wave height is greatly dependent on the starting position of the blocks, the weight of the blocks, and their porosity. The still water depth has a moderate effect on the generated wave height. The generated wave height has an impact on the overtopping volume. For some block configurations, there was no overtopping. For a small block weight, and where the starting position of the blocks is at the water's surface, there was no overtopping. With block configurations 1B and 2H, with a 31.6 mm freeboard of the dam there was no overtopping. Also, for a freeboard of 68.4 mm and the block configurations of 1B and 2H, with release heights of 0 mm and 500 mm, there was no overtopping. There was only a very small splash of water.
- In this study, the effect of porous blocks on the wave generation and overtopping volume was studied. For both solid and porous blocks, a similar wave pattern was observed; this observation is similar to the research of Ataie-Ashtiani and Nik-Khah, (2008). The generated wave amplitude ratio ($a_{\text{solid block}}/a_{\text{porous block}}$) was calculated and it is in the range of 0.88 to 1.67; which is very close to the findings of Heller and Spinneken, (2013). Where Heller and Spinneken, (2013) got a wave amplitude ratio of ($a_{blocks}/a_{granular}$) in the range of *0.43 to 1.76.* For this study, the total overtopping volume by the solid block is always larger than the total overtopping volume by the porous block. However, the maximum depth created by the solid blocks over the dam crest is less and greater than the porous blocks.
- The total overtopping volume of the water is dependent on the weight and release height of the slide blocks, on the freeboard of the dam, and on the material properties of the sliding blocks; which is similar to the study of Heller et al. (2009). With the increase of the weight and release height of the block, the overtopping volume increases. However, with the increase of the block's porosity and the freeboard of the dam, the overtopping volume will decrease.
- The maximum overtopping depth created along the dam crest was quite affected by the release height and weight of the blocks; while the impact of the freeboard of the dam on the maximum overtopping depth was moderate.
- The overtopping discharge rate and distribution of the water along the dam crest were not even. A large amount of water volume overflowed at the edge of the dam crest. Also, the highest discharge rate occurred at the edge of the dam.

- Finally, the maximum overtopping depth along the dam crest and the total overtopped water volume was compared to the equation developed by Kobel et al., (2017). As per the comparison result in this study, the actual maximum overtopping depth over the dam crest is quite close to the maximum overtopping depth calculated by Kobel et al., (2017) except for few results. However, Kobel et al., (2017) overestimated the total overtopping volume. The ratio of ($V_{Kobel}/V_{measured}$) falls in the range of 1.46 to 2.7. This means the overtopping volume calculated by Kobel et al., (2017) is (*1.5 to 2.7*) times greater than the actual overtopped water volume.

7.2 Recommendation

I suggest that future experiments should be carried out with fully granular materials. This will allow a better understanding of the real situation of an earth material slide into a reservoir. Furthermore, I recommend an experimental study to be performed that shows the effect of the location of the sliding plane concerning the location of the dam structure. This may help to study the worst scenario of the location of the landslide and to quantify the degree of damage. In this physical model, the sliding plane has a constant slope; I suggest performing experimental studies by varying the slope of the sliding plane, which will allow the study of the effect of a wider range of impact velocity. Finally, I recommend experimental studies to be carried out with different basin geometry to investigate its impact on wave generation and the overtopping volume of water.

References

Abebe, B., Dramis, F., Fubelli, G., Umer, M., Asrat, A., 2010. Landslides in the Ethiopian highlands and the Rift margins. Journal of African Earth Sciences 56, 131–138.

Ataie-Ashtiani, B., Nik-Khah, A., 2008. Impulsive waves caused by subaerial landslides. Environmental Fluid Mechanics 8, 263–280.

Biedermann, J., 2015. Overtopping of embankment dams from landslide generated waves 128.

Bolzoni, M., n.d. Physical model study on impacts of landslide generated wave action on embankment dams 75.

Broothaerts, N., Kissi, E., Poesen, J., Van Rompaey, A., Getahun, K., Van Ranst, E., Diels, J., 2012. Spatial patterns cause and consequences of landslides in the Gilgel Gibe catchment, SW Ethiopia. CATENA 97, 127–136.

Evers, F., Hager, W., 2015. Impulse Wave Generation: Comparison of Free Granular with Mesh-Packed Slides. Journal of Marine Science and Engineering 3, 100–110.

Fritz, H.M., Hager, W.H., 2003. Landslide generated impulse waves. Experiments in Fluids 35, 505–519.

Gaurina-Medjimurec, N. (Ed.), 2015. Handbook of Research on Advancements in Environmental Engineering: Advances in Environmental Engineering and Green Technologies. IGI Global.

GENEVOIS, R., 2013. THE VAJONT LANDSLIDE: STATE-OF-THE-ART. Italian Journal of Engineering Geology and Environment 15–39.

Gohari, M., Avarideh, A., 2018. The Effect of Landslide at Dam Reservoirs on Seismic Behavior of Earth Dams 14.

Heller et al., 2009.

Heller, V., Spinneken, J., 2015. On the effect of the water body geometry on landslide–tsunamis: Physical insight from laboratory tests and 2D to 3D wave parameter transformation. Coastal Engineering 104, 113–134.

Heller, V., Spinneken, J., 2013. Improved landslide-tsunami prediction: Effects of block model parameters and slide model. Journal of Geophysical Research: Oceans 118, 1489–1507.

Kobel, J., Evers, F.M., Hager, W.H., 2017. Impulse Wave Overtopping at Rigid Dam Structures. Journal of Hydraulic Engineering 143, 04017002.

Landslides Mudslides, 2008. The Landslide Blog.

McFall, B.C., Fritz, H.M., 2016. Physical modelling of tsunamis generated by three-dimensional deformable granular landslides on planar and conical island slopes. Proc Math Phys Eng Sci 472.

Ponziani, L., Gardoni, M., n.d. Landslide generated waves in dam reservoirs 149.

R, G., M.i, G., 2005. The 1963 Vaiont Landslide. Giornale di Geologia Applicata.

Skrzypczak, I., Kokoszka, W., Kogut, J., 2017. The Impact of Landslides on Local Infrastructure and the Environment,

Supervision of dams - NVE [WWW Document], 2015.

Take, W.A., Mulligan, R.P., 2017. LANDSLIDE GENERATED WAVES: NEW INSIGHTS FROM PHYSICAL MODELS 4.

Tang, G., Lu, L., Teng, Y., Zhang, Z., Xie, Z., 2018. Impulse waves generated by subaerial landslides of combined block mass and granular material. Coastal Engineering 141, 68–85.

Tekeze Dam, Ethiopia | International Rivers [WWW Document], 2008.

Woldearegay, K., 2013. Review of the occurrences and influencing factors of landslides in the highlands of Ethiopia: With implications for infrastructural development 5, 29.

Appendix A

Comparison of maximum overtopping depth with Kobel, Evers and Hager (2017) equation

The value of maximum overtopping depth is compared to the Kobel equation developed in 2017. The result of the comparison is presented in Table A-0-1 for porous blocks and Table A-0-2 for solid blocks. In Table A-0-1and Table A-0-2 the value marked red is data which doesn't fulfill Kobels requirement. It is not used for comparison in this study. The value of E should be $0.1 < E2 < 0.75$ while the value of ε should be o.1 to 0.7 for freeboard of 23.7mmand 31.6mm. while foe freeboard of 68.4mm, it should be $0.2 < \varepsilon < 0.7$.

Table A-0-1 Comparison of measured value of maximum overtopping depth to calculated value using Kobel formula for porous blocks.

Freeboard (mm)	Block arrangement	Release height (mm)	Wave amplitude (mm)	Still water depth (mm)	Dam Height (mm)	β	ε	E2	do/w =1.32E2	Maximum overtopping depth		Relative error (%)
										Calculated value	Measured value	
23.68	1B	1500	29.29	295	318.68	33.69	0.10	0.06	0.08	25.55	33.64	31.65
	1B	1000	26.56	295	318.68	33.69	0.09	0.05	0.07	23.11	30.26	30.98
	1B	500	21.42	295	318.68	33.69	0.07	0.04	0.06	18.54	24.54	32.35
	1B	0	16.78	295	318.68	33.69	0.06	0.03	0.04	14.45	10.41	-27.93
	4B	500	33.30	295	318.68	33.69	0.11	0.07	0.09	29.18	34.41	17.92
	4B	0	32.72	295	318.68	33.69	0.11	0.07	0.09	28.65	29.86	4.22
	2V	500	23.30	295	318.68	33.69	0.08	0.05	0.06	20.20	34.14	68.97
	2V	0	20.16	295	318.68	33.69	0.07	0.04	0.05	17.42	19.22	10.34
	2H	500	30.07	295	318.68	33.69	0.10	0.06	0.08	26.26	29.51	12.37
	2H	0	20.94	295	318.68	33.69	0.07	0.04	0.06	18.11	9.47	-47.73
31.57	1B	1500	31.27	287	318.68	33.69	0.11	0.06	0.08	24.87	30.68	23.35
	1B	1000	27.31	287	318.68	33.69	0.10	0.05	0.07	21.60	30.68	42.07
	1B	500	27.47	287	318.68	33.69	0.10	0.05	0.07	21.72	16.98	-21.84
	1B	0	15.88	287	318.68	33.69	0.06	0.03	0.04	12.35	6.06	-50.90
	4B	500	30.36	287	318.68	33.69	0.11	0.06	0.07	24.11	27.92	15.82
	4B	0	32.42	287	318.68	33.69	0.11	0.06	0.08	25.82	23.47	-9.12

	2V	500	22.16	287	318.68	33.69	0.08	0.04	0.05	17.39	29.27	68.27
	2V	0	19.97	287	318.68	33.69	0.07	0.04	0.05	15.63	16.85	7.83
	2H	500	26.41	287	318.68	33.69	0.09	0.05	0.06	20.86	25.72	23.29
	2H	0	20.63	287	318.68	33.69	0.07	0.04	0.05	16.15	9.07	-43.82
68.42	1B	500	28.28	250	318.68	33.69	0.11	0.03	0.04	13.97	3.75	-73.16
	2H	500	31.96	250	318.68	33.69	0.13	0.04	0.05	16.01	4.22	-73.68
	2V	500	36.15	250	318.68	33.69	0.14	0.04	0.06	18.41	11.43	-37.90
	4B	500	41.20	250	318.68	33.69	0.16	0.05	0.07	21.39	14.34	-32.96

Table A-0-2 Comparison of measured value of maximum overtopping depth to calculated value using Kobel formula for solid blocks.

Freeboard (mm)	Block arrangement	Release height (mm)	Wave amplitude (mm)	Still water depth (mm)	Dam Height (mm)	β	ε	E2	do/w =1.32E2	Maximum overtopping depth		Relative error (%)
										Calculated value	Measured value	
23.68	1B	1500	33.31	295	318.68	33.69	0.11	0.07	0.09	29.19	33.64	15.24
	1B	1000	28.06	295	318.68	33.69	0.10	0.06	0.08	24.45	30.26	23.76
	1B	500	22.69	295	318.68	33.69	0.08	0.05	0.06	19.66	24.54	24.78
	1B	0	17.17	295	318.68	33.69	0.06	0.03	0.05	14.79	10.41	-29.61
	4B	0	46.34	295	318.68	33.69	0.16	0.10	0.13	41.16	29.86	-27.46
	2V	0	30.49	295	318.68	33.69	0.10	0.06	0.08	26.64	19.22	-27.84
	2H	0	27.35	295	318.68	33.69	0.09	0.06	0.07	23.81	9.47	-60.24
31.57	1B	1500	43.99	287	318.68	33.69	0.15	0.08	0.11	35.65	30.68	-13.93
	1B	1000	37.94	287	318.68	33.69	0.13	0.07	0.09	30.47	30.68	0.69
	1B	500	26.52	287	318.68	33.69	0.09	0.05	0.06	20.95	16.98	-18.94
	1B	0	18.29	287	318.68	33.69	0.06	0.03	0.04	14.27	6.06	-57.51
	4B	0	46.38	287	318.68	33.69	0.16	0.09	0.12	37.71	23.47	-37.76
	2V	0	31.57	287	318.68	33.69	0.11	0.06	0.08	25.12	16.85	-32.91
	2H	0	28.24	287	318.68	33.69	0.10	0.05	0.07	22.36	9.07	-59.41
68.42	1B	500	31.07	250	318.68	33.69	0.12	0.04	0.05	15.51	3.75	-75.83
	2H	500	46.77	250	318.68	33.69	0.19	0.06	0.08	24.82	4.22	-83.01
	2V	500	41.23	250	318.68	33.69	0.16	0.05	0.07	21.42	11.43	-46.61
	4B	500	61.45	250	318.68	33.69	0.25	0.08	0.11	34.52	14.34	-58.45

Appendix B

Calibration

One of the instruments which needs calibration is the overtopping collecting buckets. To measure the volume of the water overtopped, the bucket must be calibrated. Frist add water to the bucket and make the level flat. After that take a reading using ultrasonic sensors shown on Figure B-0-1. After taking the first reading add known volume of water (1liter) and take the reading of the level again. Repeat this for additional 4 to 6 times and calculate the calibrating factor.

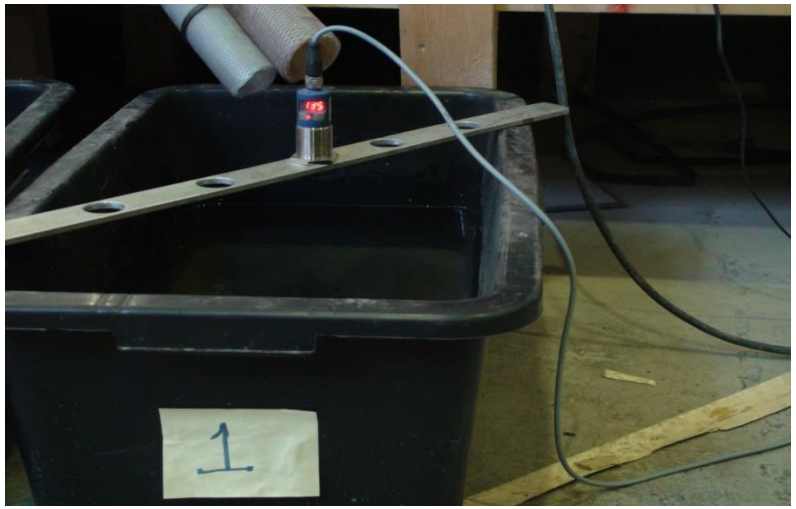

Figure B-0-1 Reading the overtopped volume of water

The other instrument that require calibration is the overtopping sensor. To calibrate the overtopping sensor, start the Agilent software and run the software to record the data. At the same time under the overtopping sensor insert known thickness of material with some time interval. The sensor records rectangular wave. The reading value due to the material is the increased value from the constant reading. Figure B-0-2 below shows the recorded data for 45mm thickness of the material. to calculate the calibration, factor the same procedure applies for all sensors. Here is the formula for sensor 12.

$$\boldsymbol{Calibration\ factor} = \left[\frac{\boldsymbol{thickness\ of\ the\ inserted\ material}}{\boldsymbol{average\ value\ of\ 'd'}}\right] = \left[\frac{\boldsymbol{45mm}}{\boldsymbol{average\ value\ of\ 'd'}}\right] \ldots\ldots\ldots\ldots\ldots\ldots\ldots\ldots\ldots\ldots\ldots\ldots\ldots\ldots \boldsymbol{A}\text{-}1$$

The overtopping depth at the crossponding time is calculated using the calibration factor. The sensor record the data every 0.05 second. To calculate overtopping depth

$$Overtopping\ depth = [calibration\ factor * recorded\ data]$$

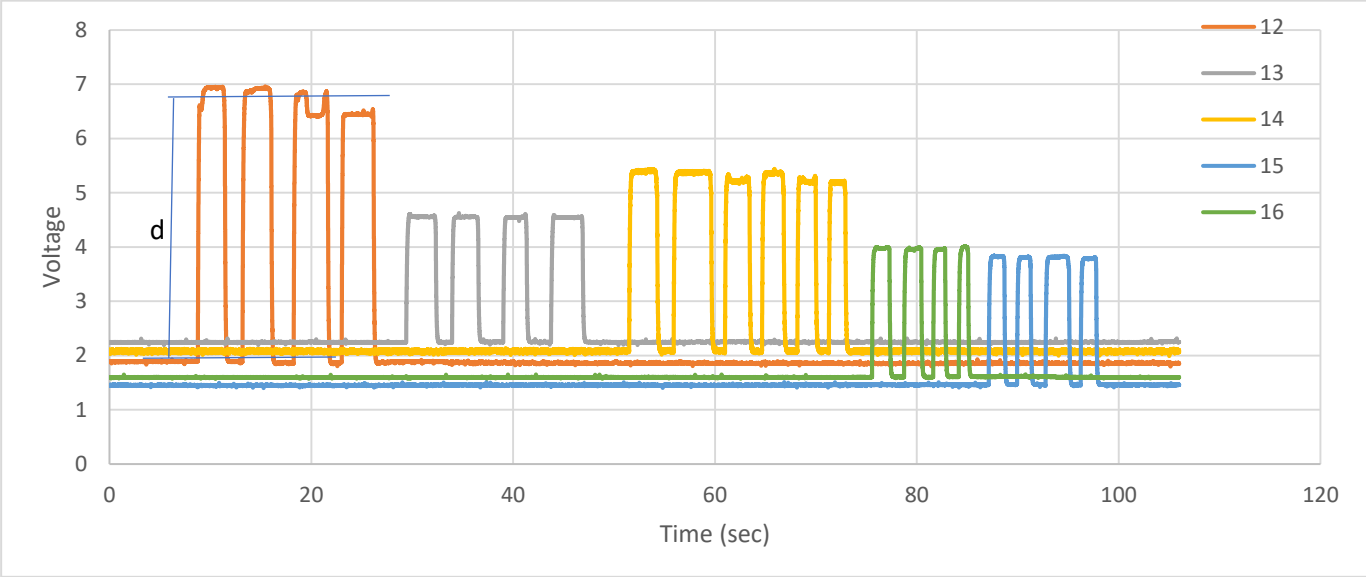

Figure B-0-2 Calibration of overtopping sensor

Appendix C

Effect of impact velocity on overtopping volume and maximum depth over the dam crest

The effect of impact velocity on overtopping volume of the water and the maximum depth created over the dam crest is similar both for porous and solid blocks.

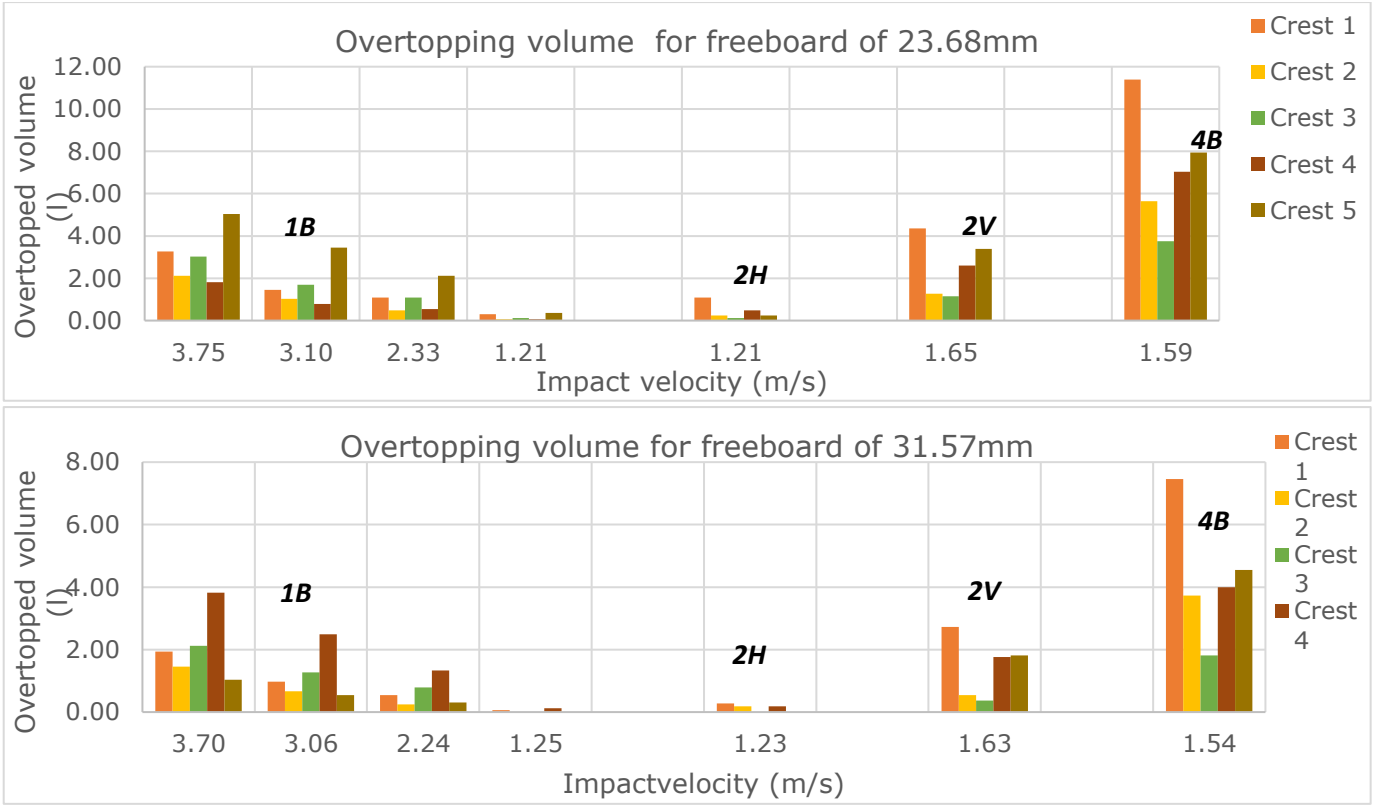

Figure C-0-3 Impact of velocity on total overtopping volume for solid blocks.

Maximum overtopping depth for porous and solid blocks with different block configuration and impact velocity. Figure C-0-4 shows effect of impact velocity on the maximum overtopping depth created for solid blocks. Figure C-0-5 shows the maximum overtopping depth created for porous blocks with different impact velocity. The graph is for both freeboard of 23.68mm and 31.57mm

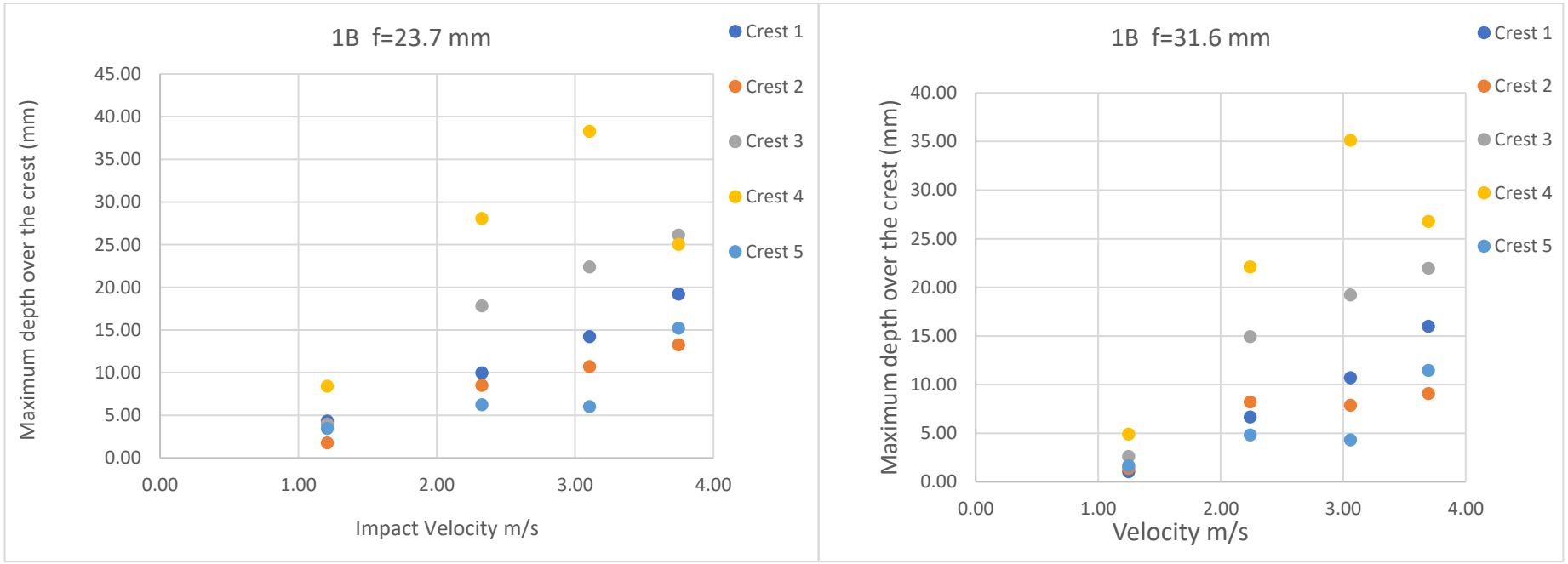

Figure C-0-4 Impact of velocity on maximum overtopping depth for solid blocks.

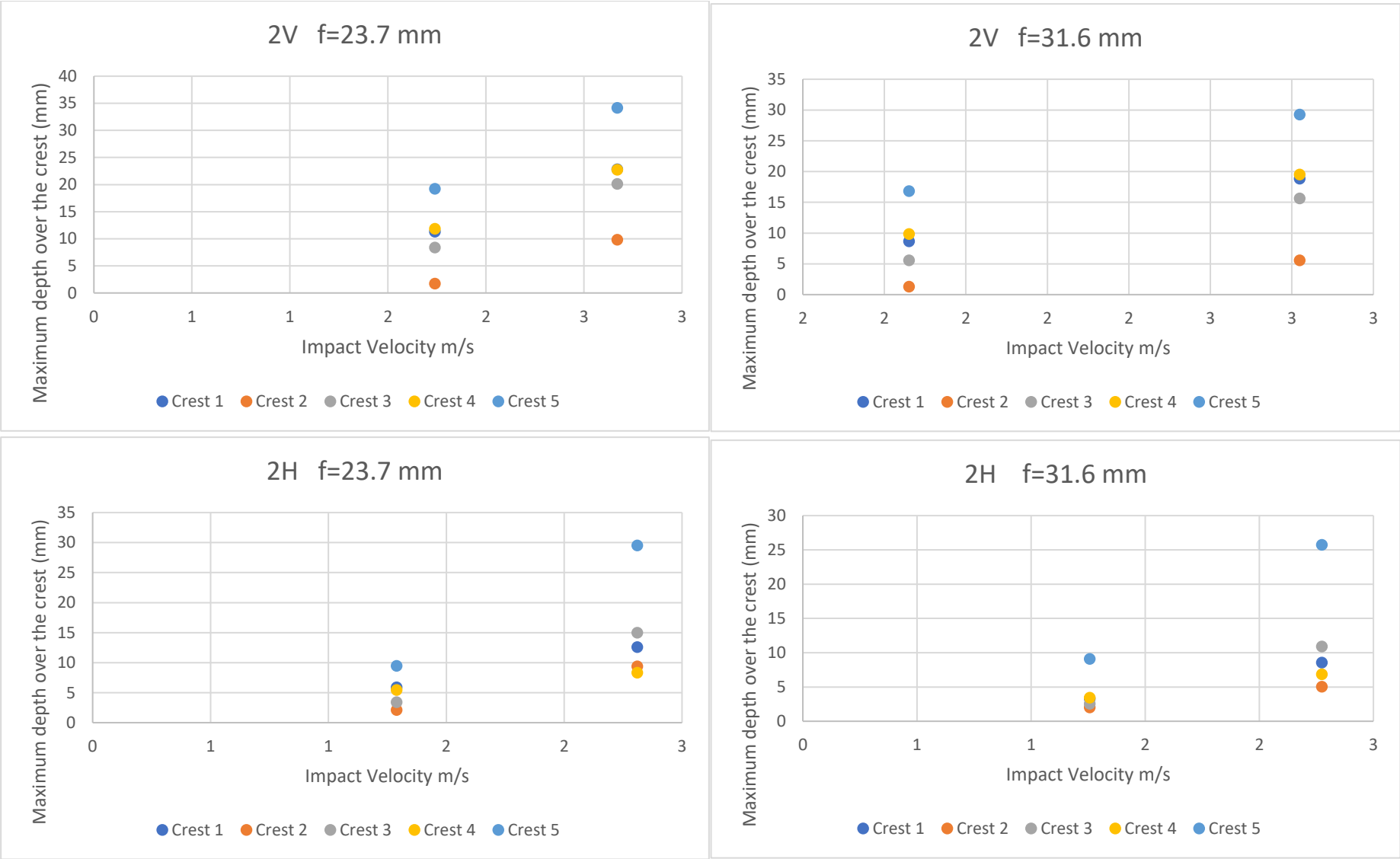

Figure C-0-5 Impact of velocity on maximum overtopping depth for porous blocks

Appendix D

Summarized wave height for the nine sensors

The below tables show the summarized wave height recorded by the nine sensors. Sensor 7 is intermittent during the test and the reading may not be correct reading. For that reason, it colored in red.

A. Porous blocks.

Table D-0-3 Wave height recorded for porous blocks with freeboard of 23.7mm of the dam

freeboard (mm)	block arrangement	Release height (mm)	Max wave height[mm]	Wave height (mm)								
				Ch. 1	Ch. 2	Ch. 3	Ch. 4	Ch. 5	Ch. 6	Ch. 7	Ch. 8	Ch. 9
4.5	1B	1500	61.83	61.83	33.59	36.37	43.75	24.27	43.90	23.33	27.92	29.29
		1000	40.82	40.82	31.00	32.77	38.32	25.51	39.23	0.00	26.56	25.57
		500	38.74	38.74	34.86	25.06	26.35	25.80	30.65	18.48	18.66	21.42
		0	25.01	25.01	18.89	19.93	16.17	18.56	22.31	10.77	15.52	16.78
	4B	500	83.55	83.55	51.98	44.56	50.77	36.95	63.05	33.30	23.97	25.61
		0	63.67	63.67	43.34	47.35	56.46	27.94	50.67	0.00	22.96	32.72
	2V	500	49.35	49.35	34.07	34.89	31.25	24.83	39.52	0.00	22.97	23.30
		0	31.44	30.95	30.78	28.49	26.30	23.31	31.44	0.00	20.16	18.86
	2H	500	55.57	44.42	55.57	32.26	32.78	41.23	39.92	0.00	30.07	23.59
		0	31.45	24.97	23.10	23.03	22.11	21.49	31.45	0.09	20.94	17.82

Table D-0-4 Wave height recorded for porous blocks with freeboard of 31.6mm of the dam

freeboard	block arrangement	Release height	Max wave height[mm]	Wave height (mm)								
				Ch. 1	Ch. 2	Ch. 3	Ch. 4	Ch. 5	Ch. 6	Ch. 7	Ch. 8	Ch. 9
6	1B	1500	50.05	50.05	36.12	33.32	47.64	23.07	42.87	23.53	29.02	31.27
		1000	39.56	39.56	31.05	31.21	37.21	23.59	36.85	24.73	27.31	22.07
		500	40.72	40.72	32.77	24.83	27.15	23.65	33.67	27.47	19.88	24.90
		0	24.05	21.65	16.26	18.69	15.67	15.89	24.05	13.90	15.88	15.67
	4B	500	83.08	83.08	56.26	42.14	53.56	35.06	63.05	30.36	24.79	26.55
		0	63.96	63.96	45.49	43.88	57.82	25.67	51.00	23.83	21.70	32.42
	2V	500	47.87	47.87	26.32	36.38	32.43	23.90	42.79	0.09	22.16	21.95
		0	34.15	32.46	24.23	29.98	28.49	21.44	34.15	0.09	19.32	19.97
	2H	500	60.38	36.90	60.38	35.49	32.18	34.60	42.89	0.09	26.41	25.93
		0	33.73	24.76	26.30	29.15	21.85	22.62	33.73	0.12	20.42	20.63

Table D-0-5 Wave height recorded for porous blocks with freeboard of 68.4mm of the dam

Freeboard	Block arrangement	Release height	Max wave height [mm]	Wave height (mm)								
				Ch. 1	Ch. 2	Ch. 3	Ch. 4	Ch. 5	Ch. 6	Ch. 7	Ch. 8	Ch. 9
13	1B	500	35.61	34.55	26.26	26.05	30.98	22.38	35.61	0.08	21.30	28.28
	2H	500	55.87	48.53	55.87	33.73	36.81	27.59	41.07	0.09	29.53	31.96
	2V	500	58.58	58.58	31.53	38.53	34.90	20.64	53.25	0.08	20.53	36.15
	4B	500	93.60	93.60	56.03	65.20	52.15	33.22	66.52	0.08	30.01	39.46

B. Solid blocks.

The below table shows the wave height recorded by solid blocks with different freeboards of the dam. The value indicated with '*' is data which is from previous students.

Table D-0-6 Wave height recorded for solid blocks with freeboard of 23.7mm of the dam

Freeboard (mm)	Block arrangement	Release height (mm)	Max wave height [mm]	Wave height (mm)								
				Ch. 1	Ch. 2	Ch. 3	Ch. 4	Ch. 5	Ch. 6	Ch. 7	Ch. 8	Ch. 9
4.5	1B	1500	58.62	58.62	53.35	41.32	48.63	42.69	51.67	22.73	33.31	21.92
		1000	45.42	45.42	39.34	33.97	36.60	37.78	40.69	20.95	27.21	28.06
		500	34.25	34.25	32.21	25.05	31.43	30.36	32.03	15.07	21.76	22.69
		0	29.85	20.94	19.25	19.12	21.92	19.25	29.85	14.93	16.02	17.17
	2H	0	44.17	37.25	44.17	24.42	39.60	29.45	35.81	14.28	27.35	25.19
		*500										
	2V	0	53.14	50.87	41.85	32.97	48.66	35.34	53.14	26.97	26.56	30.49
		*500	73.18	73.18	34.94	35.77	48.29	27.97	39.53	23.53	27.20	39.91
	4B	0	104.80	104.80	77.62	47.33	61.56	40.20	68.15	46.34	32.21	41.36
		*500	93.87	93.87	56.25	44.76	59.54	39.98	51.73	23.93	32.22	42.99

Table D-0-7 Wave height recorded for solid blocks with freeboard of 31.6mm of the dam

freeboard (mm)	block arrangement	Release height (mm)	Max wave height [mm]	Wave height (mm)

				Ch. 1	Ch. 2	Ch. 3	Ch. 4	Ch. 5	Ch. 6	Ch. 7	Ch. 8	Ch. 9
6	1B	1500	53.42	53.42	53.42	37.74	50.21	43.66	49.41	21.92	35.32	43.99
		1000	47.72	47.72	39.48	32.33	38.15	37.67	46.79	20.61	31.08	37.94
		500	36.15	36.15	35.30	28.57	31.36	26.89	33.67	14.65	26.52	21.65
		0	30.56	22.45	20.19	19.55	22.90	18.83	30.56	13.04	18.29	17.64
	2H	0	47.77	38.76	47.77	26.36	40.16	28.10	35.71	8.21	28.24	25.22
		*500										
	2V	0	53.82	53.82	43.89	37.41	48.27	34.39	52.60	19.84	24.59	31.57
		*500	64.26	64.26	38.02	39.14	42.32	25.36	42.60	21.17	26.37	43.25
	4B	0	98.57	98.57	75.20	44.39	62.22	35.35	69.59	41.64	31.02	46.38
		*500	82.06	82.06	49.08	51.60	50.67	38.46	51.42	24.14	36.63	39.63

Table D-0-8 Wave height recorded for solid blocks with freeboard of 23.7mm of the dam

freeboard (mm)	block arrangement	Release height (mm)	Max wave height [mm]	Wave height (mm)								
				Ch. 1	Ch. 2	Ch. 3	Ch. 4	Ch. 5	Ch. 6	Ch. 7	Ch. 8	Ch. 9
13	1B	500	44.87	44.87	43.08	29.31	28.37	26.59	35.33	19.88	26.95	31.07
	2H	500	72.15	72.15	59.23	49.40	41.89	31.25	44.23	24.40	30.16	46.77
	2V	500	77.05	77.05	53.72	46.91	49.26	40.98	52.25	29.22	27.46	41.23
	4B	500	127.79	127.79	81.59	76.75	71.49	50.38	68.61	61.45	36.84	49.20

Appendix E

Collected photo

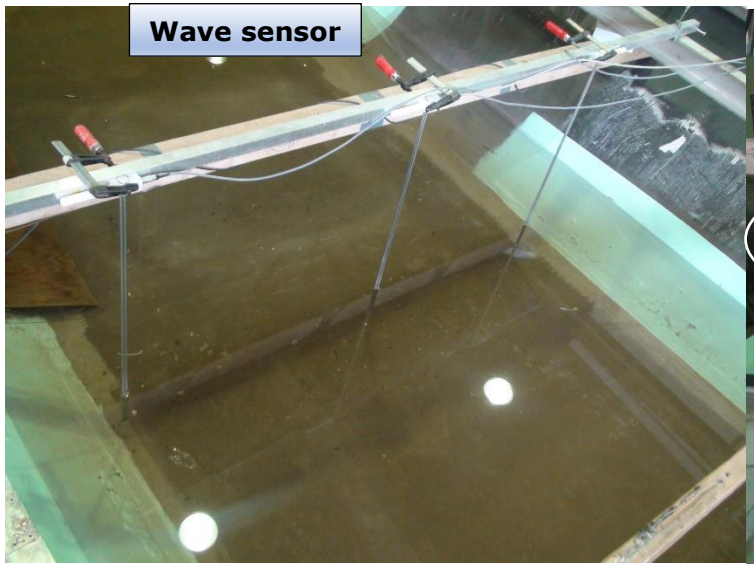

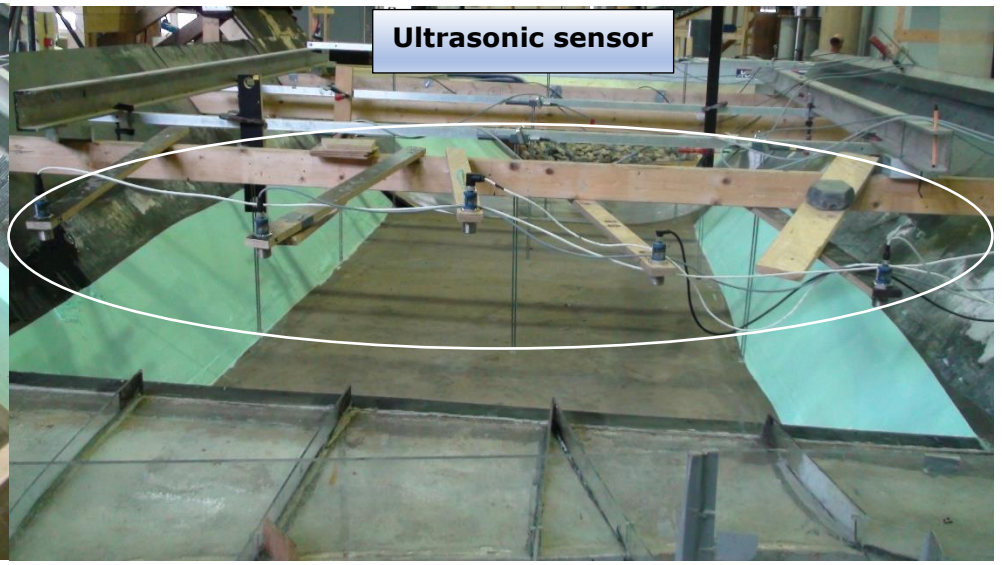

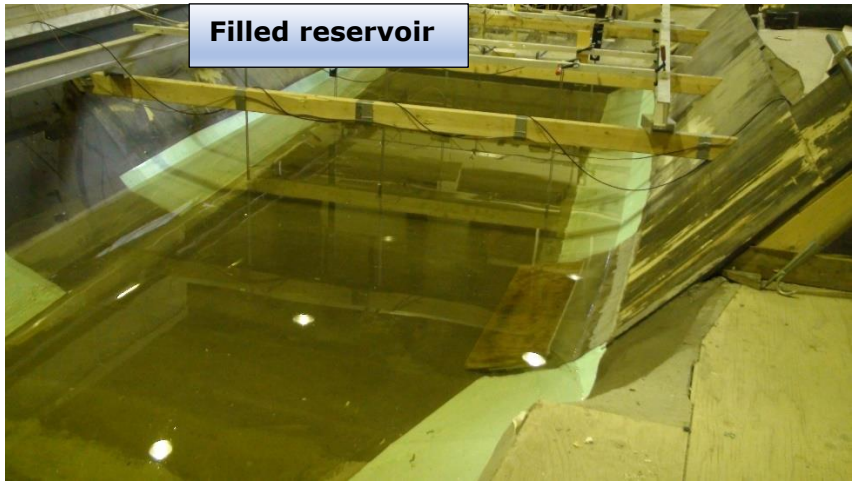

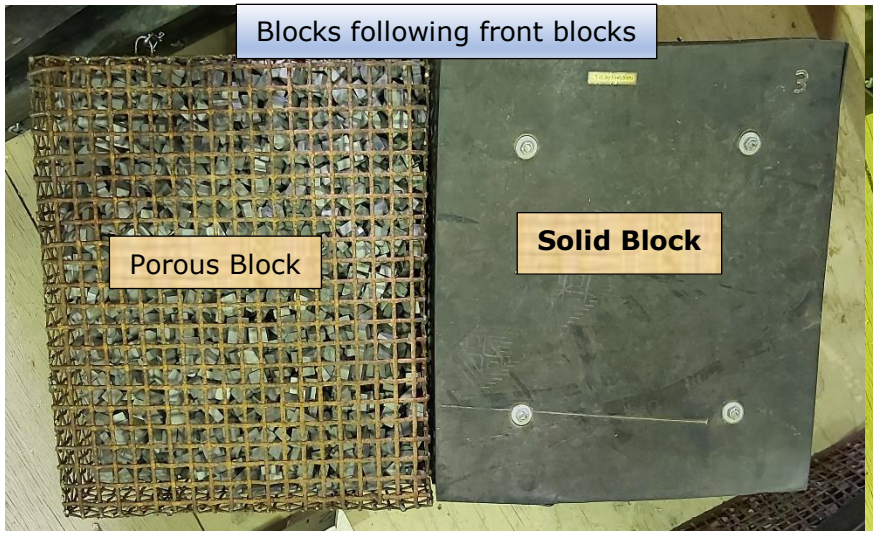
Blocks following front blocks
Porous Block
Solid Block

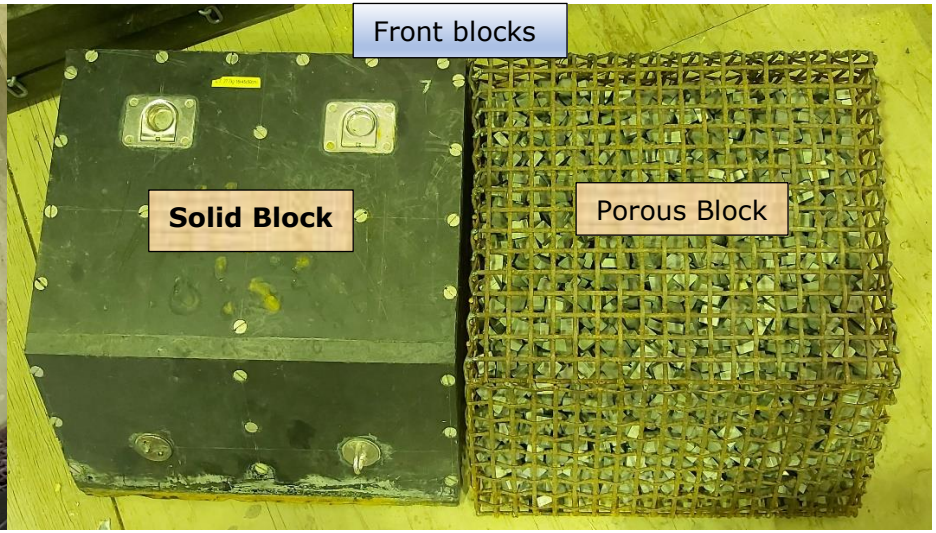
Front blocks
Solid Block
Porous Block

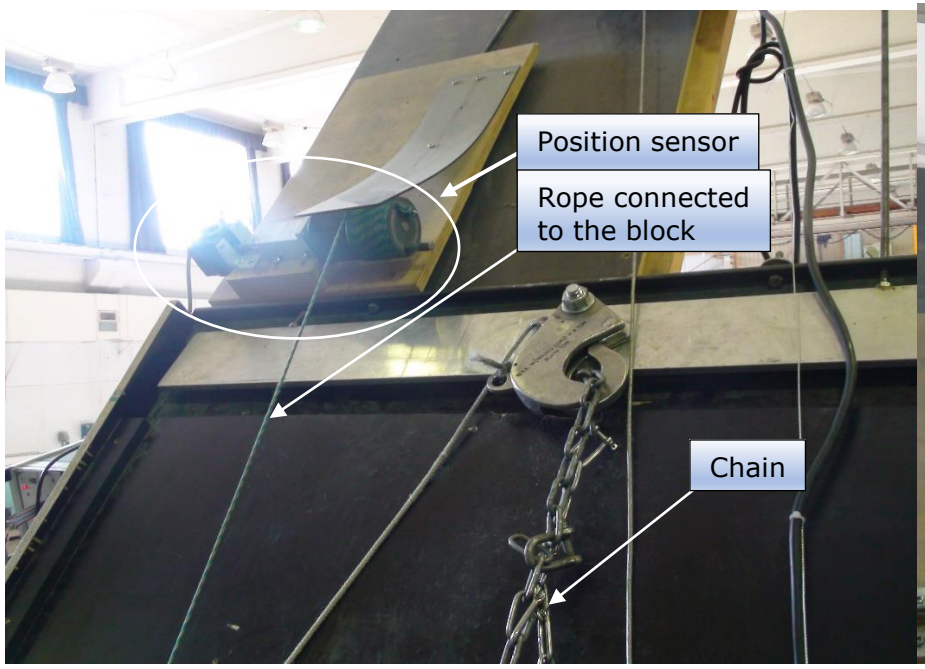
Position sensor
Rope connected to the block
Chain

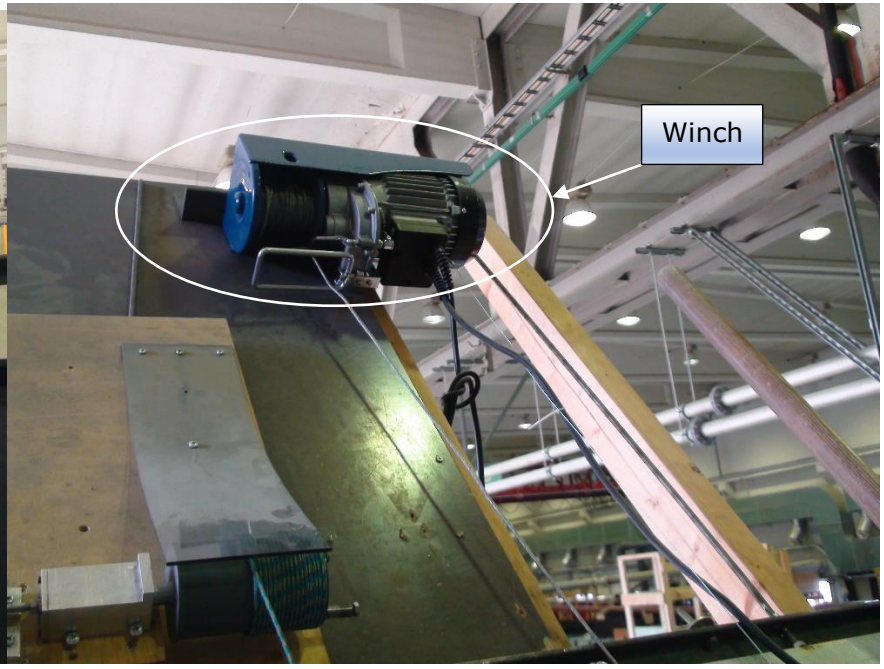
Winch

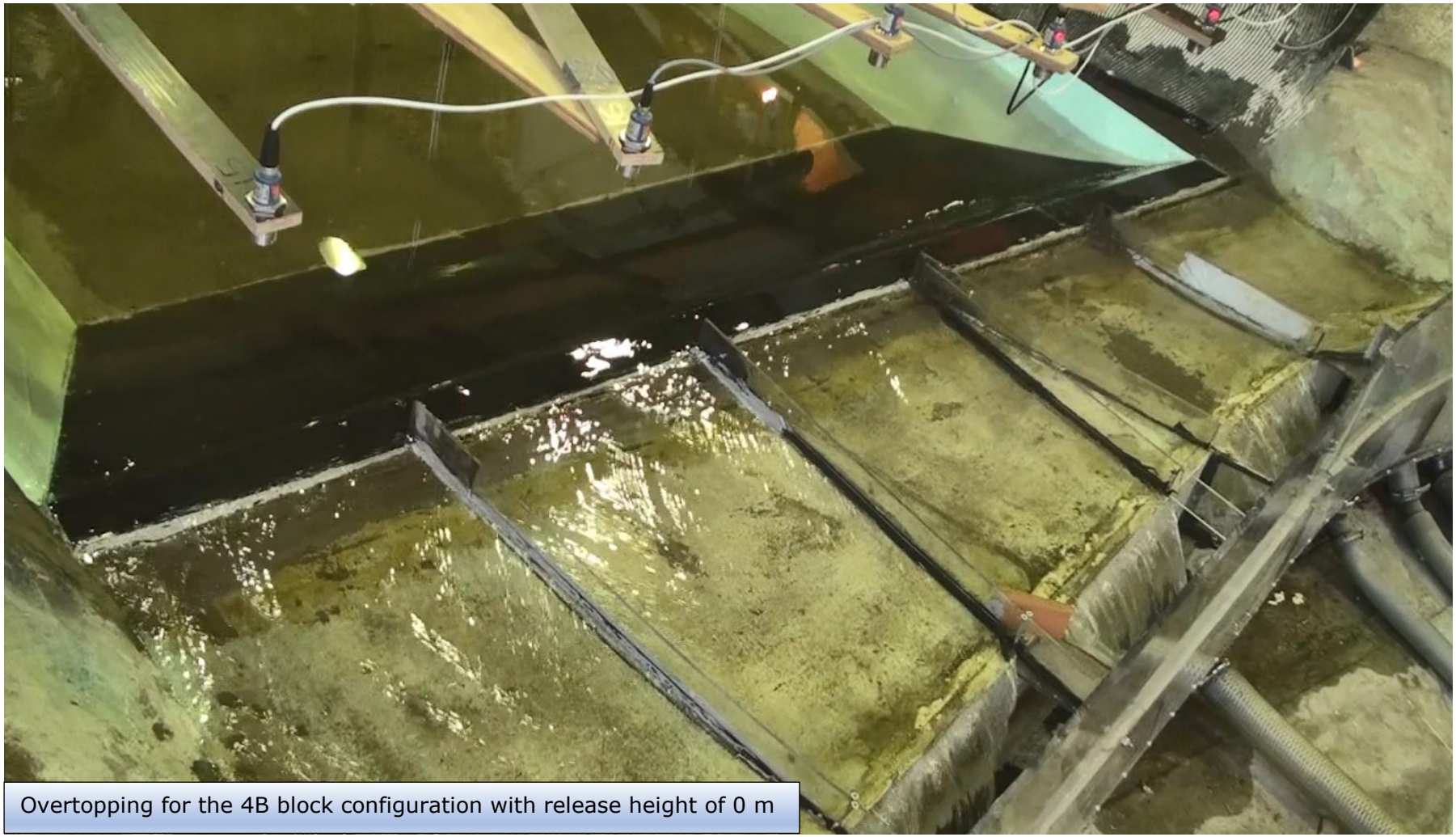

Overtopping for the 4B block configuration with release height of 0 m

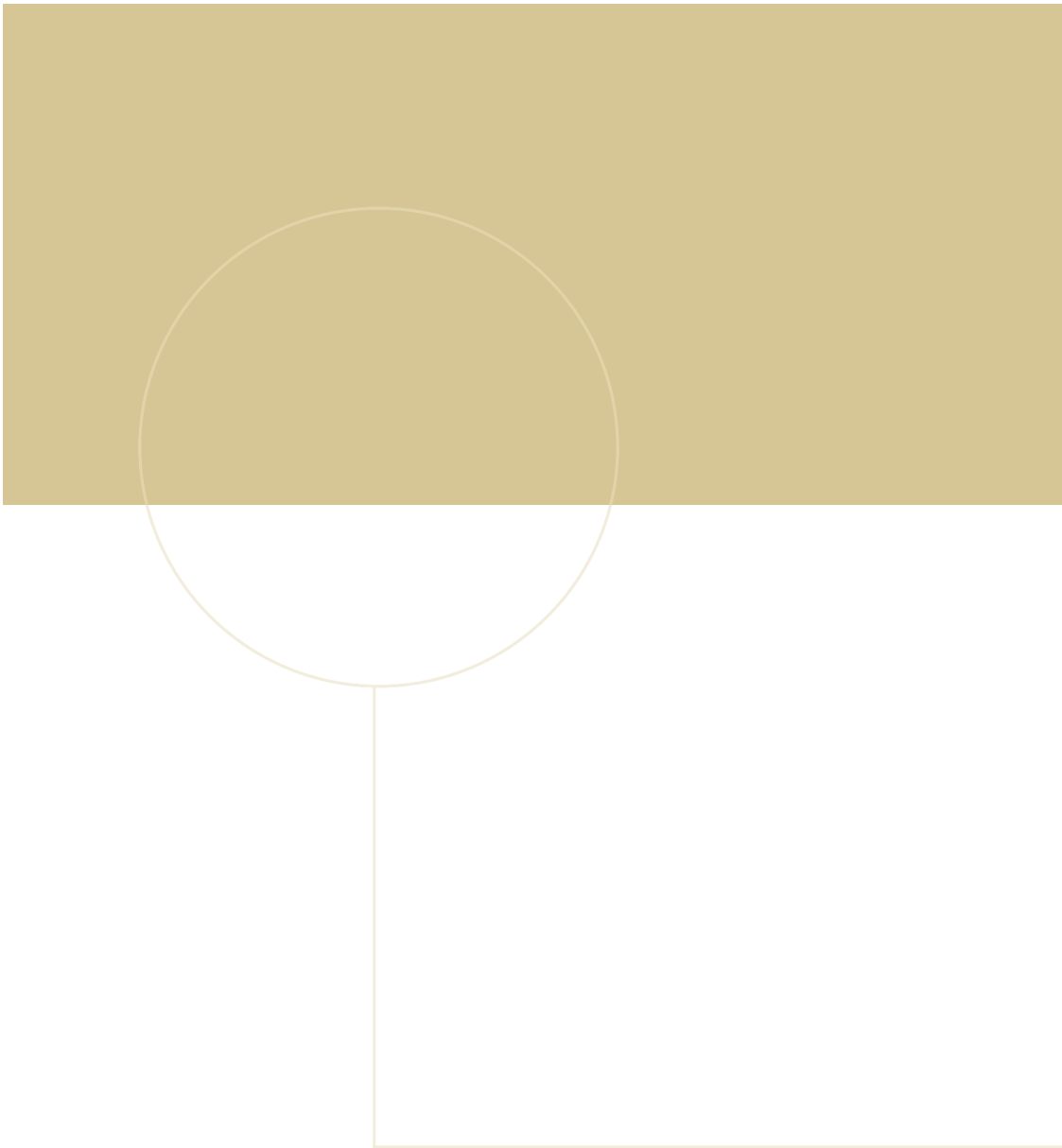

NTNU
Norwegian University of
Science and Technology